toxins

MDPI

Article

Mentha pulegium L. (Pennyroyal, Lamiaceae) Extracts Impose Abortion or Fetal-Mediated Toxicity in Pregnant Rats; Evidenced by the Modulation of Pregnancy Hormones, MiR-520, MiR-146a, TIMP-1 and MMP-9 Protein Expressions, Inflammatory State, Certain Related Signaling Pathways, and Metabolite Profiling via UPLC-ESI-TOF-MS

Amira A. El-Gazar [1], Ayat M. Emad [2], Ghada M. Ragab [3] and Dalia M. Rasheed [2,*]

[1] Pharmacology and Toxicological Department, Faculty of Pharmacy, October 6 University, Sixth of October City 12585, Egypt; amira.ahmed@o6u.edu.eg
[2] Pharmacognosy Department, Faculty of Pharmacy, October 6 University, Sixth of October City 12585, Egypt; ayatEmad@o6u.edu.eg
[3] Pharmacology and Toxicological Department, Faculty of Pharmacy, Misr University for Science & Technology (MUST), Giza 12585, Egypt; ghada.ragab@must.edu.eg
* Correspondence: daliarasheed@o6u.edu.eg; Tel.: +2-011-1673-8432

Citation: El-Gazar, A.A.; Emad, A.M.; Ragab, G.M.; Rasheed, D.M. *Mentha pulegium* L. (Pennyroyal, Lamiaceae) Extracts Impose Abortion or Fetal-Mediated Toxicity in Pregnant Rats; Evidenced by the Modulation of Pregnancy Hormones, MiR-520, MiR-146a, TIMP-1 and MMP-9 Protein Expressions, Inflammatory State, Certain Related Signaling Pathways, and Metabolite Profiling via UPLC-ESI-TOF-MS. *Toxins* **2022**, *14*, 347. https://doi.org/10.3390/toxins14050347

Received: 20 April 2022
Accepted: 13 May 2022
Published: 16 May 2022

Abstract: Pregnant women usually turn to natural products to relieve pregnancy-related ailments which might pose health risks. *Mentha pulegium* L. (MP, Lamiaceae) is a common insect repellent, and the present work validates its abortifacient capacity, targeting morphological anomalies, biological, and behavioral consequences, compared to misoprostol. The study also includes untargeted metabolite profiling of MP extract and fractions thereof *viz.* methylene chloride (MecH), ethyl acetate (EtOAc), butanol (But), and the remaining liquor (Rem. Aq.) by UPLC-ESI-MS-TOF, to unravel the constituents provoking abortion. Administration of MP extract/fractions, for three days starting from day 15th of gestation, affected fetal development by disrupting the uterine and placental tissues, or even caused pregnancy termination. These effects also entailed biochemical changes where they decreased progesterone and increased estradiol serum levels, modulated placental gene expressions of both MiR-(146a and 520), decreased uterine MMP-9, and up-regulated TIMP-1 protein expression, and empathized inflammatory responses (TNF-α, IL-1β). In addition, these alterations affected the brain's GFAP, BDNF, and 5-HT content and some of the behavioral parameters escorted by the open field test. All these incidences were also perceived in the misoprostol-treated group. A total of 128 metabolites were identified in the alcoholic extract of MP, including hydroxycinnamates, flavonoid conjugates, quinones, iridoids, and terpenes. MP extract was successful in terminating the pregnancy with minimal behavioral abnormalities and low toxicity margins.

Keywords: *Mentha pulegium* (pennyroyal); abortion; UPLC metabolite profiling; IUGR; micro-RNA; MMP-9

Key Contribution:

- Verification of *Mentha pulegium* (MP) abortifacient capacity in pregnant rats.
- UPLC-MS revealed MP profile to harbor metabolites with phytoestrogenic potential.

1. Introduction

Abortifacients are compounds that induce miscarriage or abortion, and the herbs used for such purposes, either intentionally or by misconception may pose toxicity risks to the administering mother. The use of herbs and plant extracts to intervene with pregnancy and enforce menses is one ancient folk practice that entails complex social, legal, ethical, and health aspects [1].

Plants of genus Mentha (Lamiaceae) are aromatic, medicinal, and ornamental herbaceous plants with a wide distribution all over the world as they can flourish in diverse habitats. Varieties of Mentha are extensively used in food, cosmetics, and in aroma and in complementary therapies, primarily for the treatment of gastrointestinal complaints, such as indigestion, flatulence, spasm, nausea, irritable bowel syndrome, and ulcerative colitis [2]. *Mentha pulegium* L. (Pennyroyal) is an aromatic perennial herb of the mint family with a strong spearmint-like odor. Earlier it was widely cultivated and used traditionally as an insect repellent, food preservative, emmenagogue, and to relieve menstruation ailments [3]. However, its distribution and use have declined remarkably in recent years, because of pennyroyal toxicity claims to humans, especially regarding its pulegone rich essential oil [4,5]. One of the earlier traditional practices pertained to pennyroyal consumption was to terminate undesired pregnancies or to expel dead fetuses [6]. In fact, the use of pennyroyal infusion as a natural abortifacient has been repeatedly reported, even Carl Linnaeus, listed pennyroyal as an abortifacient in his 1749 Materia medica [1,6,7]. However, the mechanism of pregnancy termination/ abortion and correlating this action to pennyroyal's metabolic profile has yet to be investigated. According to the phytochemical investigations, the chemical composition of pennyroyal can be divided into two major groups; water-soluble phytoconstituents viz. phenolic acids, flavonoids and dihydrochalcone glycosides in addition to lipophilic fatty acids and terpene derivatives [8]. Flavonoid compounds previously reported in pennyroyal include derivatives of quercetin, isorhamnetin, naringenin, and gallocatechins, whereas hydroxycinnamic acid derivatives include rosmarinic and salvianolic acid conjugates signifying the Lamiaceae members [9].

Misoprostol is currently the drug of choice for induction of medical abortion as a single regimen in many regions where mifepristone is not indexed/unreachable or expensive, in addition to the convince in its use/administration [10–12]. Misoprostol is a prostaglandin E1 analogue with a wide range of applications, particularly in obstetrics and gynecology [13]. Misoprostol induces abortion through raising uterine tone and contractions in pregnant women [13,14]. However, misoprostol unsuccessful attempt may be associated with fetal deformity, and congenital abnormalities, and the reasons surrounding these effects are still vague and requires more investigation [15,16].

The scientific progress towards characterizing the role of natural product involvement in jeopardizing pregnancy and unrevealing the pharmacological action and psychological consequences is still very limited. This research can be regarded as a decisive endeavor for settling the potential abortifacient capacity of MP extract by unraveling the underlined mechanistic pathway and analyzing the incidences associated with its intended and/or misuse in comparison to misoprostol. Considering that the failure of early pregnancy termination, through folk practice or medical procedures, is associated with increased incidence of a variety of disorders inflected on the mother and fetus, hence tracking the congenital abnormalities, teratogenicity, biological, behavioral, and pathological consequences is momentous.

2. Results

2.1. Dose Selection

2.1.1. Abortifacient and Biochemical Effects of Different Doses of *Mentha pulegium* L. Body Weight-Related

Administration of *Mentha pulegium* L. extract in a dose of 250 and 500 mg/kg resulted in complete abortion of two of the six pregnant rats relative to the effect of the standard drug misoprostol (three of the six rats), whereas 125 mg/kg revealed less effectiveness as it did not show a complete abortion among its group. However, the 125 mg/kg dose resulted in a reduction in progesterone levels and showed signs of toxicity viz. asymmetric distribution of fetuses in the two uterine horns, absorption points, hematoma, and absence of boundaries between fetal balls; presented in Table 1, Figure 1 (panel I) as red brackets, green arrows, star, and yellow arc, respectively.

Table 1. Effect of different doses (125, 250, and 500 mg/kg) of 70% ethanol extract of *Mentha pulegium* L. on the abortifacient parameters and serum progesterone in pregnant rats.

Group		No. of Completely Aborted Rats/Group	Abortion %	No. of Fetus Remaining	Serum Progesterone
Pregnant		0/6	0	11–12	22.5
Misoprostol 100 ug/kg		3/6	50%	7–8	9.8 [a]
Plant Extract dose	125 mg/kg	0/6	0	8–9	18.7 [a,b]
	250 mg/kg	2/6	33%	7–8	11.7 [a]
	500 mg/kg	2/6	33%	7–8	10.5 [a]

Values are presented as mean ($n = 6$) ± SD and statistical analysis was carried out using one-way ANOVA followed by Tukey's post hoc multiple comparison test. As compared with control (a), misoprostol (b); $p < 0.05$.

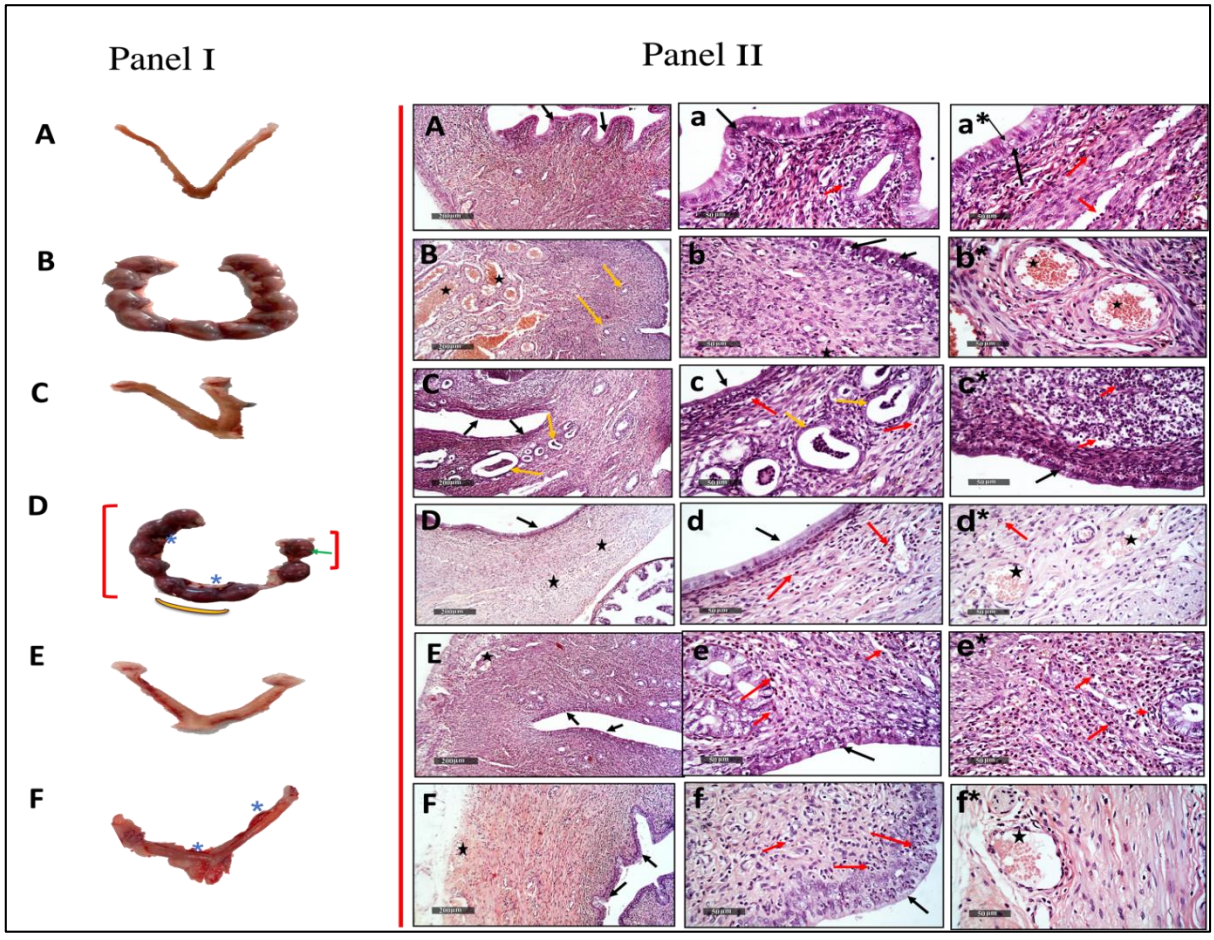

Figure 1. Representative images of the female rat uterus dissected on the 18th day of gestation. (**C**) misoprostol, and (**E**,**F**) MP (extract; 250, 500 mg/kg, respectively) uterus with complete abortion but (**F**) with additional appearance of intensive bleeding and hemorrhage (star) as compared to: (**A**) normal uterus presentation of unmated female rat, and (**B**) uterus with normal fetal distribution and normal physiological appearance of pregnancy. However (**D**) showed no complete abortion but asymmetric distribution of fetuses in the two uterine horns: red brackets; resorption points: green arrows; hematoma: star; and absence of boundaries between fetal balls: yellow arc (**Panel I**). Photomicrographs images of histopathological uterine tissue alterations after hematoxylin and eosin staining; (**A**,**a**,**a***) un-mated/control negative, (**B**,**b**,**b***) pregnant/control positive, (**C**,**c**,**c***) misoprostol, (**D**,**d**,**d***), (**E**,**e**,**e***), and (**F**,**f**,**f***) MP extract 125, 250, and 500 mg/kg, respectively. (**Panel II**).

2.1.2. Histopathological Effects of the Different Doses of *Mentha pulegium* L. on Uterine Tissues

The paraffin sections as imaged in Figure 1(IIB) pregnant uterine tissue revealed more thickening of the uterine wall with mild vacuolization of lining epithelium (black arrow), as well as mild hyperplasia of uterine gland (yellow arrow) and many dilated and congested blood vessels of intermuscular tunica vascular (star) in pregnant rats as compared tox Figure 1(IIA) non-pregnant rats that demonstrated the apparent intact uterine wall with almost intact lining epithelium with scattered apoptotic cell bodies (black arrow) moderate submucosal mononuclear cells infiltrates (red arrow) alternated with normal connective tissue and intact myometrium, as well as normal intermuscular blood vessels (star). Furthermore, treatment with different doses of the MP extract presented an order in efficacy/power, that was augmented by increasing the extract dose, where Figure 1(IID) 125 mg/kg of MP showed mild endometritis with mild neutrophilic infiltrates (red arrow), as well as mild congested uterine vasculatures (star). The Figure 1(IIE) MP 250 mg/kg dose demonstrated more apparent endometritis with moderate vacuolar changes of lining uterine epithelium (black arrow). Eventually, Figure 1(IIF) MP 500 mg/kg dose showed the worst histo-findings where significant hyperplasia of lining epithelium (black arrow) with many intra epithelial inflammatory cells infiltrates with milder infiltrates (red arrow) in submucosal layers and mild congested uterine BVs (star) and abundant neutrophilic infiltrates (red arrow) with mild congested uterine BVs (star) were observed as compared to medically aborted rats using Figure 1(IIC) misoprostol that manifested significant atrophy of lining epithelium (black arrow), cystic dilatation of many endometrial glands with abundant intraluminal desquamated lining epithelium (yellow arrow) accompanied with sever endometritis and lymphocytic infiltrates (red arrow).

2.1.3. Acute Toxicity Test

No deaths were observed. However, at the dose level of 500 mg/kg, signs of toxicity on uterine tissue were observed as mentioned previously.

2.2. Identification of the Abortifacient Mechanism of MP Extract and Fractions Thereof

2.2.1. Abortifacient Effects/Activities of 250 mg/kg and Different Fractions of *Mentha pulegium* L.

Rats treated with MP extract or misoprostol behaved similarly in terms of the number of completely aborted rats, the change in weight of pregnant rats/mothers and the number and weights of remaining fetuses relative to positive control mothers and healthy fetuses (Table 2, Figure 2I). On the other hand, the different fractions did not show complete abortion, but a significant reduction in fetal weight was observed, and was more pronounced with the but. and remaining aqueous fractions showing the maximum weight reduction in mothers on 18th day compared to the 15th day of gestation and the highest intrauterine growth retardation (IUGR) detected by fetal weight. Additionally, the MP and different fractions generated a different pattern of toxicity on uterine tissue, as shown in Figure 2(II), such as hematoma, intensive bleeding, asymmetrical distribution of fetuses in the two horns of uterus, complete absence of fetus on one uterine horn, resorption sites, absence of boundaries between fetal balls, and small fetal balls. Panel III presents IUGR associated with Figure 2(IIIb) misoprostol Figure 2(IIIc) MP extract and its fractions administration, as implied by their weights and lengths, morphologic malformations, hematoma, transparency of skin, and intensive bleeding as compared to those of fetuses in Figure 2(IIIa) control group. We omitted the fetal lengths measurements although there was significant difference between groups as high elasticity and flexibility of fetus may be a misleading during measurements and increase error.

Table 2. Effect of the 70% ethanol extract of *Mentha pulegium* L. and fractions thereof on the abortifacient parameters and serum progesterone in pregnant rats.

Group	No. of Completely Aborted Rats/gp	Abortion %	No. of Fetus Remaining
Pregnant	0/6	0	12–13
Misoprostol (ST)	2/6	33%	6–8
MP (250 mg/kg)	2/6	33%	6–9
MecH (125 mg/kg)	0/6	0	7–11
EtOAc (125 mg/kg)	0/6	0	7–11
But. (125 mg/kg)	0/6	0	3–8
Rem. aq. (125 mg/kg)	0/6	0	2–6

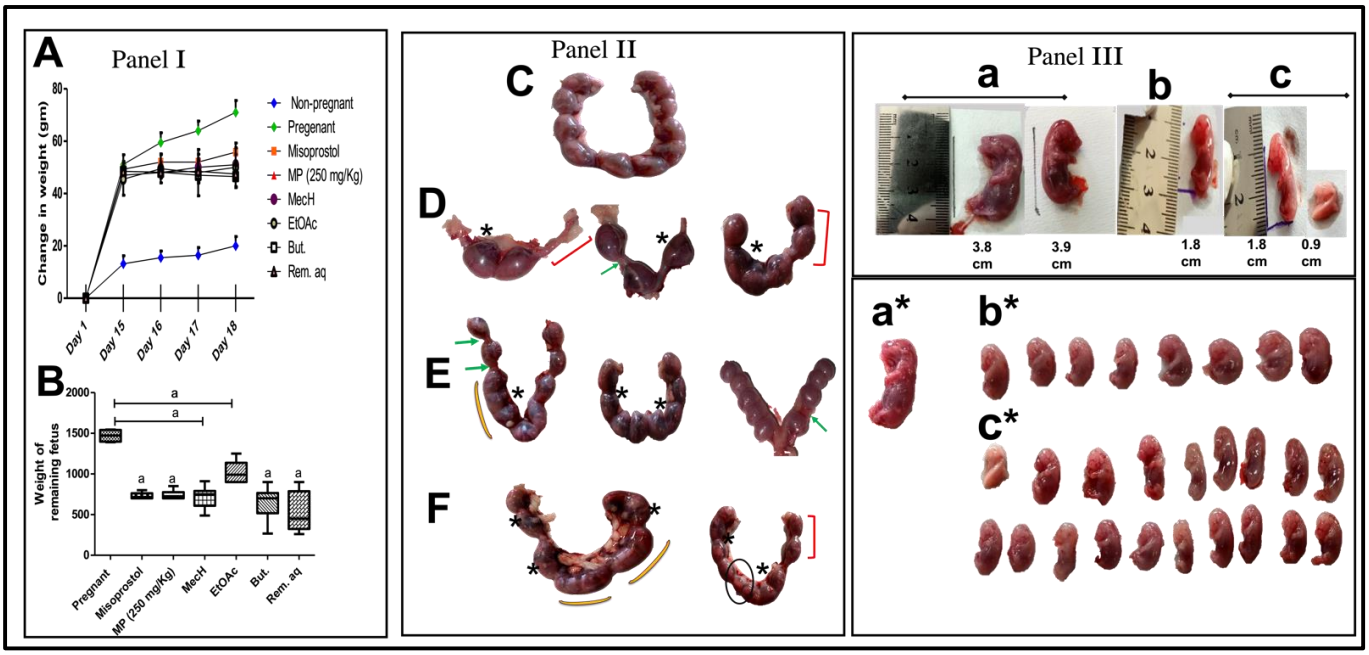

Figure 2. (**A**) change in weight of pregnant rats in different groups as compared to unmated/unpregnant female through the study (days: 1st, 15th, 16th, 17th, and 18th of gestation), and (**B**) weight of remaining fetus (**Panel I**). (**A**) Two-Way RM ANOVA with one factor repetition (time: day) was utilized to analyze the change in rat weight and (**B**) the non-parametric data of fetal weight were expressed as the median (min-max) and were analyzed using the non-parametric Kruskal–Wallis followed by Dunn's as the post hoc test and student *t* test (**Panel I**). Common pathological observations and features of uterine tissues. (**C**) Pregnant rats with normal fetal distribution in the two horns; (**D**–**F**) MP (extract/fraction) or misoprostol on the 18th day of gestation. Observations: (**D**); the uterus with asymmetrical distribution of fetuses in the two horns, complete absence of fetus in one horn, remarkable resorption sites, and reduced number of fetal balls, (**E**,**F**); asymmetrical distribution of fetuses in the two horns, absence of boundaries between fetal balls, reduced sized fetal balls, notable resorption sites, and intensive bleeding. The asymmetric distribution of fetuses in the two uterine horns: red brackets; resorption points: green arrows; hematoma: star; and absence of boundaries between fetal balls: yellow arc; reduced fetal balls: black circle (**Panel II**). MP (extract or fractions) and Misoprostol-mediated structural abnormalities in fetus including height, weight, and physical appearance; (**a**,**a***) pregnant, (**b**,**b***) Misoprostol, and (**c**,**c***) MP; extract or fractions groups respectively (**Panel III**).

2.2.2. Effect of *Mentha pulegium* L. on the Serum Levels of Progesterone and Estradiol

As shown in Figure 3I, pregnant female rats treated with misoprostol (100 ug/kg) and 250 mg/kg of MP extract both, had a marked decline in serum Figure 3(IA) progesterone levels and this effect reached Figure 3(IB) estradiol levels which was increased as compared to untreated pregnant female rats. It is worth mentioning that both MP extract and the standard drug, misoprostol produced similar values, where the progesterone levels were 11.17 ± 1.6 and 9.70 ± 2.0 ng/mL and the estradiol levels were 76.30 ± 3.0 and 72.55 ± 7.0 pg/mL, respectively. Meanwhile, the different fractions of MP extract also exhibited an abortifacient effect by the observed decline in serum progesterone levels. Additionally, the butanol and the remaining aqueous fractions effectively increased the levels of estradiol as compared to healthy pregnant one and those treated with total extract.

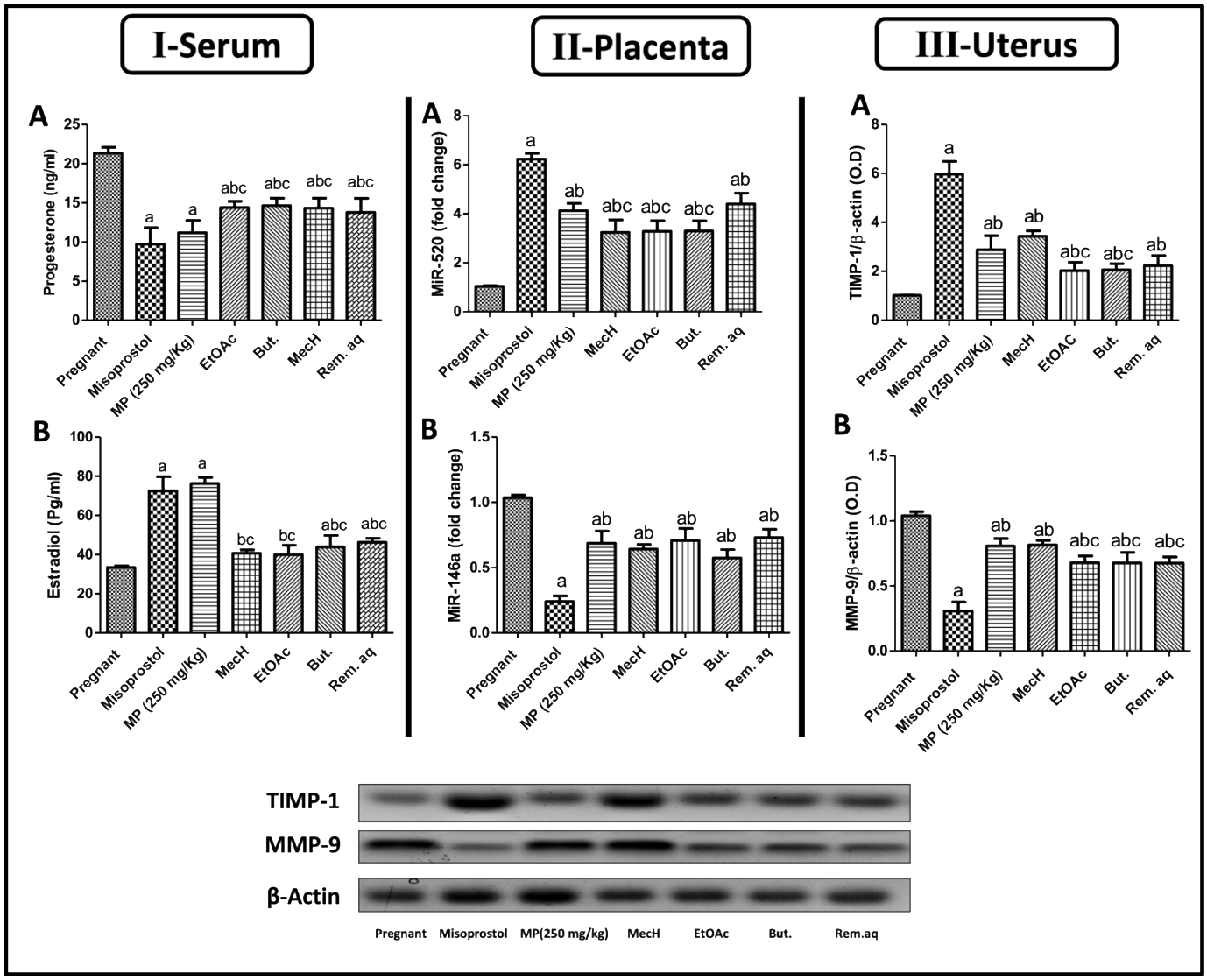

Figure 3. The serum levels of (**A**) progesterone and (**B**) estradiol (**Panel I**). Placental protein expression of (**A**) MiR-520 and (**B**) MiR-146a (**Panel II**). Uterine protein expression of (**A**) TIMP-1**,** (**B**) MMP-9 (**Panel III**). Values are presented as mean (n = 6) ± SD and statistical analysis was carried out using one-way ANOVA followed by Tukey's post hoc multiple comparison test. As compared with control (a), misoprostol (b), MP (c); $p < 0.05$. But.: butanol; EtOAc: ethyl acetate; MecH: methylene chloride; MiR-520: micro ribonucleic acid-520; MiR-146a: micro ribonucleic acid-146a; MMP-9: matrix metalloproteinase-9; MP: *Mentha pulegium* L.; TIMP-1: tissue inhibitor matrix metalloproteinase-1; Rem. aq.: remaining aqueous.

2.2.3. Effect of *Mentha pulegium* L. on Placental Protein Expressions of MiR-520 and MiR-146a

Figure 3II illustrates the disturbance in micro-RNA (MiR) expression in all the pregnant rats after misoprostol or MP (extract; 250 mg/kg) treatment where both increased Figure 3(IIA) MiR-520 and decreased Figure 3(IIB) MiR-146a protein expression as compared to the pregnant ones. Furthermore, these perturbations in both MiRs' expression were also figured in groups of the different fractions, knowing that Rem.aq. showed the highest increase in MiR-520 among fractions as compared to MP values, however all the fractions showed almost the same inhibitory effect as the total extract on MiR-146a.

2.2.4. Effect of *Mentha pulegium* L. on Uterine Protein Expressions of MMP-9 and TIMP-1

As revealed in Figure 3III, a marked elevation in Figure 3(IIIA) TIMP-1 that in sequence decreased Figure 3(IIIB) MMP-9 protein expression was detected on treatment with misoprostol or MP extract as compared to untreated pregnant female. Furthermore, medically aborted rats by our chosen standard showed a higher effect on the uterine TIMP-1 and MMP-9 expression as compared to values of MP extract. Regarding the fractions, they showed similar activity to total MP extract on TIMP-1 and MMP-9 expression with the MecH fraction exhibiting the highest effect on TIMP-1 and MMP-9 expressions, whereas the Rem. aq. fraction was more dominant on TIMP-1 expression.

2.2.5. Effect of *Mentha pulegium* L. on Serum Inflammatory Markers

Figure 4I depicts the effect of MP extract administration on the levels of inflammatory mediators, Figure 4(IA) tumor necrosis factor alfa (TNF-α) and Figure 4(IB) interlukin-1 beta (IL-1β) which were emphatically spiked after its administration for three days and even exceeding them misoprostol effects on TNF-α levels (29.80% and 56.17% of control pregnant rats, respectively). Furthermore, the inflammatory activity of all the fractions under investigation were confirmed by the elevated inflammatory markers as compared to MP extract. Nevertheless, the Rem. Aq. Fraction recorded the highest increase in TNF-α among all the animals to reach 76.67% of normal pregnant ones. Concerning IL-1β, the But. And Rem. Aq. Fractions gave no significant difference compared to MP extract which marks a more significant effect in accordance with their employed doses.

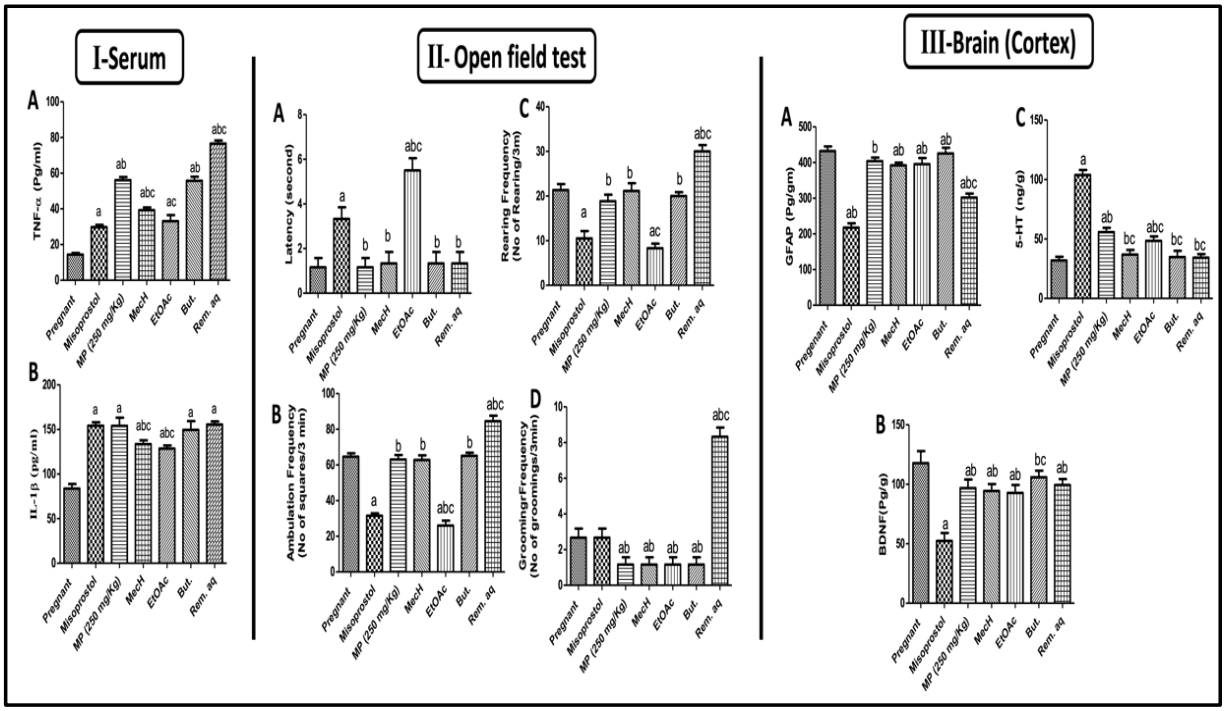

Figure 4. The serum levels of (**A**) TNF-α and (**B**) IL-1β (**Panel I**). The behavioral changes in an open

field test on (**A**) latency time, (**B**) rearing frequency, (**C**) number of squares crossed/3 min, and (**D**) grooming frequency (**Panel II**). Cortical contents of (**A**) GFAP, (**B**) BDNF, and (**C**) 5-HT (**Panel III**). Values are presented as mean (n = 6) ± SD and statistical analysis was carried out using one-way ANOVA followed by Tukey's post hoc multiple comparison test. As compared with control (a), misoprostol (b), MP (c); $p < 0.05$. BDNF: brain derived neurotrophic factor; But.: butanol; EtOAc: ethyl acetate; GFAP: Glial fibrillary acidic protein; 5-HT: 5-Hydroxytryptamine; IL-1β: interlukin-1beta; MecH: methylene chloride; MP: *Mentha pulegium* L.; Rem. Aq.: remaining aqueous, TNF-α: tumor necrosis factor-alfa.

2.2.6. Effect of *Mentha pulegium* L. on Behavioral Changes in Open Field Test

In the open field test (Figure 4II), female rats behaved differently after misoprostol, MP, and different fraction administration, indicating a variety of behavioral abnormalities associated with medically induced abortion. The ones treated with misoprostol and EtOAc fraction showed immobilization for Figure 4(IIA) 3 and 5 s., respectively, as represented by increase in the time from putting the animal into the middle of the device until its first movement (latency time), reflecting a defect in motor function by decreasing locomotor activity as compared to the untreated pregnant female. However, the MP extract and the other fractions *viz.* MecH, But. And Rem.aq. showed no latency lag compared to the control rats. The increased Figure 4(IIA) latency time in both misoprostol and EtOAc fraction was reflected on and extended to Figure 4(IIB) ambulation and Figure 4(IIC) rearing frequencies, where both showed reduced records relevant to MP extract and other fractions except the Rem.aq. fraction. This exceptional increase in rearing and ambulation frequency occurring by the Rem.aq. fraction treatment, may reflect anxiety and stress. The MP extract and its fractions reduced Figure 4(IID) grooming frequency, except for the Rem.aq. fraction treated group, which showed a significant increase in the number of times of rapid cleaning movements of the forelegs towards the face and/or the body (licking the fur, washing the face, or scratching behavior).

2.2.7. Effect of *Mentha pulegium* L. on Cortical GFAP, BDNF, and 5HT-3 Levels

Misoprostol treatment affected the brain where a decreased in cortical contents of Figure 4(IIIA) GFAP was detected. Surprisingly, MP treatment on day 15th of gestation and for three days saved GFAP levels in cortical brain tissue and showed comparable levels of GFAP to the positive control. Additionally, all the fractions exerted the same effect of MP extract except for the Rem.aq. fraction which demonstrated a marked decline in GFAP levels as compared to MP extract results. However, all the rats when compared to the positive control demonstrated a significant reduction in cortical Figure 4(IIIB) BDNF levels after misoprostol and MP extract and/or fractions treatments; where all the fractions showed similar patterns with no statistical difference when compared to their corresponding extract except for But. The fraction did not affect BDNF levels showing the same values of control pregnant rat. It is worth mentioning that the decline in BDNF content by misoprostol treated group reached almost half of contents of the control group. Ultimately, Figure 4(IIIC) 5HT cortical contents were massively increased in misoprostol and MP extract treated rats as compared to the positive control. However, all the fractions did not affect serotonin levels except EtOAc fraction which caused a significant increase in its levels as compared to the ones with normal gestation. These results were recapitulated in Figure 4III.

2.3. Metabolite Profiling of Mentha pulegium L. *(Pennyroyal) Extract Using UPLC-ESI-TOF-MS*

UPLC–ESI–TOF-MS was employed for metabolome characterization of *Mentha pulegium* L. (MP, pennyroyal) and fractions thereof in a holistic, untargeted manner and correlate its phytochemical configuration to the anticipated abortifacient effect. The analytical procedure adopted herein warranted an adequate elution of the analytes within 30 min in an order of decreased polarity (Figure 5). A total of 128 metabolites were detected in the 70% ethanol extract of pennyroyal, classified according to their phytochemical

structures into hydroxycinnamates, several flavonoid conjugates, quinones, iridoids, and terpenes. A Tandem mass experiment was useful in distinguishing between O/C attached flavonoid and phenolic conjugates. Generally, the *O*-glycosyl attachment can be readily identified in MS^2 spectra by the neutral losses of 162, 146, and 132 amu indicative of hexose, deoxyhexose or pentose moieties, respectively, whereas the fragmentation pattern of the *C*-glycosyl conjugates shows major fragment ions resulting from neutral losses of 90 and 120 amu of pentose and hexose sugars, respectively [17].

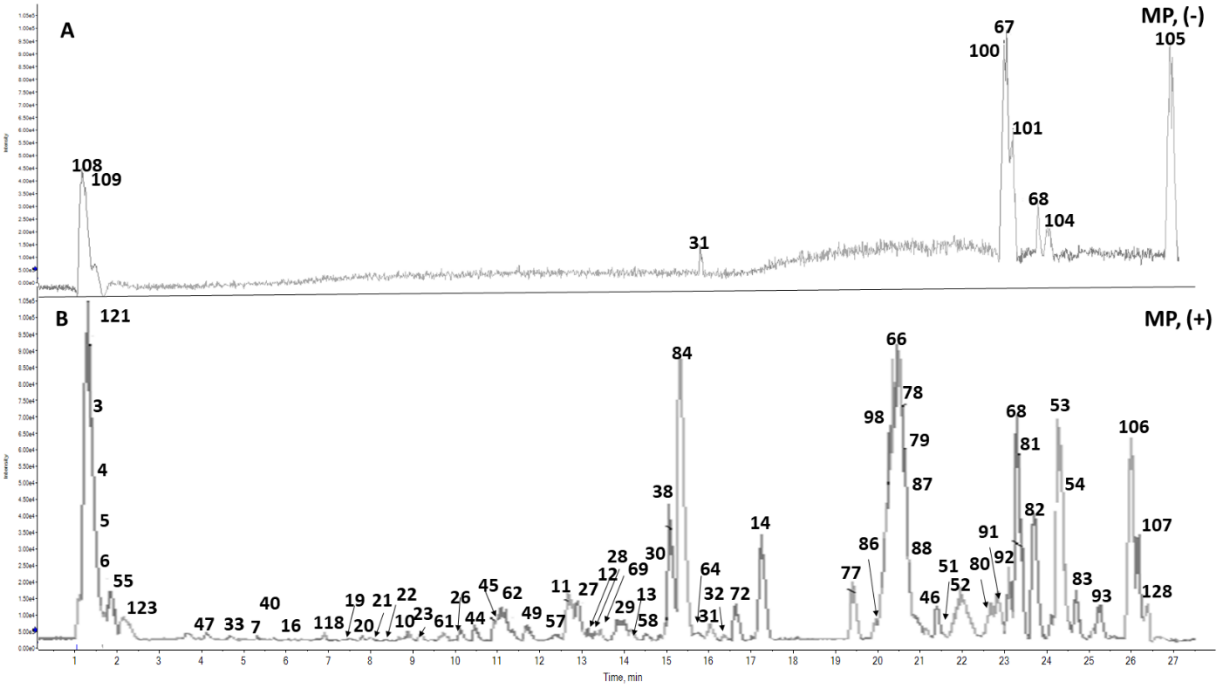

Figure 5. Representative UPLC-ESI-TOF-MS base peak chromatograms of 70% ethanol extract of *Mentha pulegium* L. (**A**), (−): negative ESI mode and (**B**), (+): positive ESI mode. Peak numbers follow metabolites listed in Table 3.

Details for detection and assigning major metabolites, listed in Table 3 and depicted in Figures 5 and 6, are explained in the following section.

Table 3. Metabolites tentatively identified in the 70% ethanol extract of (*Mentha pulegium* L.) and its fractions methylene chloride (MecH), ethyl acetate (EtOAc), butanol (But) and remaining liquor (Rem. aq.) via UPLC-ESI-TOF-MS in both; negative/positive ESI ionization modes.

Peak #	RT. (min.)	Metabolite Name	Mol. Ion *m/z*		Mass (ppm)	Elemental Composition	MS^2 Ions *m/z* (−)/(+)	Fractions
			$[M-H]^-$	$[M+H]^+$				
	Hydroxycinnamic acids and derivatives							
1	1.31	Caffeic acid-*O*-glucuronide	355.0852		−5.2	$C_{15}H_{16}O_{10}$	193, 161	
2	1.33	Caffeic acid	179.0561		0.3	$C_9H_8O_4$	161	EtOAc, Rem. aq.
3	1.49	Ferulic acid		195.0856	0.8	$C_{10}H_{10}O_4$	177, 109	MecH, Rem. aq
4	1.58	Caffeic acid dimer	341.1071	343.0823	−2.2/3.2	$C_{18}H_{14}O_7$	179, 161/181, 163	EtOAc
5	1.87	Sinapoyl-*O*-hexoside		387.1408	1.9	$C_{17}H_{22}O_{10}$	255, 169	Rem. aq
6	1.89	Cinnamic acid		149.0949	4.1	$C_9H_8O_2$	121, 65	
7	5.17	Ethyl caffeate		209.0811	1.4	$C_{11}H_{12}O_4$	191, 166	
8	7.26	Salvianolic acid K		557.1252	−6	$C_{27}H_{24}O_{13}$	363, 345	But.
9	8.82	Caffeoyl-*O*-sinapoylquinic acid	559.1422		−4.3	$C_{27}H_{28}O_{13}$	490, 354, 287	MecH, EtOAc
10	8.98	Salvianolic acid F		315.0836	−7.8	$C_{17}H_{14}O_6$	209, 179, 167	Rem. aq
11	12.55	Rosmarinic acid		361.0907	−2.9	$C_{18}H_{16}O_8$	331, 313	MecH, EtOAc
12	13.30	Caftaric acid		313.2372	7.8	$C_{13}H_{12}O_9$	295, 272, 259, 137	EtOAc
13	14.42	Methyl rosmarinate		375.1082	1.9	$C_{19}H_{18}O_8$	360, 345, 197	EtOAc
14	18.03	Rosmarinic acid derivative		379.2811	−2	$C_{23}H_{38}O_4$	361, 319, 165	EtOAc

Table 3. *Cont.*

Peak #	RT. (min.)	Metabolite Name	Mol. Ion *m/z*		Mass (ppm)	Elemental Composition	MS^2 Ions *m/z* (−)/(+)	Fractions
			$[M-H]^-$	$[M+H]^+$				
		Flavones and derivatives						
15	4.87	Apigenin-6,8-di-*C*-hexoside	593.1489		3.5	$C_{27}H_{30}O_{15}$	473, 353	Rem. aq, EtOAc
16	5.18	Penduletin-4′-*O*- glucuronide		521.1812	−1.5	$C_{24}H_{24}O_{13}$	503, 345, 327, 253	EtOAc
17	7.15	5-Hydroxy-6,7,4′-trimethoxyflavone (Salvigenin)	327.2178		3.6	$C_{18}H_{16}O_6$	190, 171	MecH
18	7.36	Apigenin-7-*O*-rutinoside (Isorhoifolin)	577.1605		9.1	$C_{27}H_{30}O_{14}$	464, 269	But.
19	7.67	Unknown apigenin glycoside		563.1752	−1.3	$C_{27}H_{30}O_{13}$	401, 383, 271	But.
20	7.79	Diosmetin-7-*O*-rutinoside (Diosmin)	607.1656	609.1782	−2.4/−0.3	$C_{28}H_{32}O_{15}$	299/463, 301	But.
21	7.85	Luteolin-7-*O*-glucuronide		463.0899	6.1	$C_{21}H_{18}O_{12}$	446, 287	
22	8.52	Apigenin-7-*O*-glucuronide	445.0776	447.0827	−7.3/1.1	$C_{21}H_{18}O_{11}$	269, 175/271	MecH, But.
23	9.35	Acacetin-7-*O*-rutinoside (Linarin)		593.1876	1.9	$C_{28}H_{32}O_{14}$	447, 285	But., Rem. aq
24	10.11	5,6,7-Trihydroxy-flavone (Baicalein)	269.0448		1.1	$C_{15}H_{10}O_5$		But., MecH
25	10.32	Pedalitin tetraacetate	483.0909		−2.6	$C_{24}H_{20}O_{11}$	336, 309	EtOAc
26	10.42	5,7,3′-trihydroxy-4′-methoxyflavone (Diosmetin, 4′-Methylluteolin)	299.0927	301.1382	−1.5/2.1	$C_{16}H_{12}O_6$	284, 151/283	But.
27	13.11	5,7-Dihydroxy-4′,6-dimethoxyflavone (Pectolinarigenin)		315.0857	−2.1	$C_{17}H_{14}O_6$	300, 282, 254	Rem. aq
28	14.02	5,4′-Dihydroxy-3,6,7-trimethoxyflavone (Penduletin)		345.0946	−6.6	$C_{18}H_{16}O_7$	330, 315, 197	MecH
29	14.23	5,7-Dihydroxy-4′-methoxyflavone (Acacetin)	283.0611	285.0753	3.5/−1.5	$C_{16}H_{12}O_5$	268, 151/242, 153	MecH
30	15.33	5-hydroxy-3,7,3′,4′-tetramethoxyflavone (Retusin)		359.1128	0.8	$C_{19}H_{18}O_7$	326, 162	EtOAc, Rem. aq
31	16.41	5-Hydroxy-3,3′,4′,6,7-pentamethoxyflavone (Artemetin)	387.1095	389.1230	5.2/−0.3	$C_{20}H_{20}O_8$	340, 319/359, 341	EtOAc, But., Rem. aq
32	16.88	5-hydroxy-7,4′-dimethoxy-6,8-dimethylflavone (Eucalyptin)		327.1252	8.0	$C_{19}H_{18}O_5$	277, 137	But., Rem. aq
		Flavanone and Flavanol derivatives						
33	5.07	Naringenin-7-*O*-glucuronide		449.1112	7.6	$C_{21}H_{20}O_{11}$	357, 273, 181	
34	5.37	Isosakuranetin-*O*-rutinoside (Didymin)		595.2831	3.6	$C_{28}H_{34}O_{14}$	577, 457	
35	5.93	Hesperetin	301.2005		−1.5	$C_{16}H_{14}O_6$	283, 255	But.
36	8.16	Eriodictyol-7-*O*-glucuronide	463.0990		3.2	$C_{21}H_{20}O_{12}$	354, 286, 218	But.
37	13.09	Sakuranetin	285.0781		8	$C_{16}H_{14}O_5$	267, 164	But.
38	15.45	Taxifolin		305.0845	8.3	$C_{15}H_{12}O_7$		
39	21.51	Hesperetin-7-*O*-rutinoside (hesperidin)		611.2864	−7.5	$C_{28}H_{34}O_{15}$	567, 538	
		Prenyl flavones						
40	5.66	Prenyl pinocembrin		325.1398	1.4	$C_{20}H_{20}O_4$	307, 191	
41	7.24	Prenyl kaempferol	353.2329		1.9	$C_{20}H_{18}O_6$	285	
42	7.93	7-O-methyl isoxanthohumol		369.1311	−5.9	$C_{22}H_{24}O_5$		
43	8.21	7,4′-Di-*O*-methyl isoxanthohumol		383.184	−3.4	$C_{23}H_{26}O_5$	365, 233	
44	10.88	Isoxanthohumol		355.1521	−5.3	$C_{21}H_{22}O_5$	267, 163	
45	14.99	Prenyl naringenin	339.216	341.1379	6.5/−1.3	$C_{20}H_{20}O_5$	309, 265	
46	21.76	Dorsmanin F		441.1897	−2.5	$C_{25}H_{28}O_7$		
		Isoflavone						
47	4.35	Daidzein-8-*C*-hexoside		417.1302	−4.6	$C_{21}H_{20}O_9$	267, 255	But., Rem. aq
		Flavonols						
48	7.35	Myricetin-3-*O*-glucuronide		495.2094	4.1	$C_{21}H_{18}O_{14}$	319, 301, 283	EtOAc
49	11.44	3,5,7,3′,4′,5′-Hexahydroxy-flavone (Myricetin)	317.0562	319.0758	−2.7/0.6	$C_{15}H_{10}O_8$	225, 164/151	
		Biflavonoid						
50	18.88	Di-*O*-methylamentoflavone (Ginkgetin)	565.1129	567.1288	0.3/0.3	$C_{32}H_{22}O_{10}$	297, 283, 165	Rem. aq
51	21.59	Amentoflavone-7,4′,4‴-trimethyl ether (Sciadopitysin)	579.1275	581.1424	−1.8/−3.2	$C_{33}H_{24}O_{10}$	297	MecH
52	22.62	4′-Monomethylamentoflavone (Bilobetin)		553.2685	−3.6	$C_{31}H_{20}O_{10}$	335, 473	Rem. aq
53	24.06	Unknown biflavonoid		647.2296	3.2	$C_{39}H_{34}O_9$	629	
54	24.98	Isochamaejasmin		543.1318	4.9	$C_{30}H_{22}O_{10}$	381, 322, 122	

Table 3. *Cont.*

Peak #	RT. (min.)	Metabolite Name	Mol. Ion *m/z*		Mass (ppm)	Elemental Composition	MS^2 Ions *m/z* (−)/(+)	Fractions
			$[M-H]^-$	$[M+H]^+$				
Quinones								
55	11.49	Przewaquinone C		297.1134	4.1	$C_{18}H_{16}O_4$	279, 261	Rem. aq
56	12.76	Przewaquinone A		311.1283	1.7	$C_{19}H_{18}O_4$		EtOAc, Rem. aq
57	12.78	Tanshinone IIA		295.1339	3.5	$C_{19}H_{18}O_3$	277, 149	MecH, Rem. aq
58	15.07	Przewaquinone F		313.1075	1.5	$C_{18}H_{16}O_5$	277, 259, 149	Rem. aq
		Iridoids						
59	5.54	Loganic acid		377.1466	6.4	$C_{16}H_{24}O_{10}$		MecH
60	5.66	Aucubin		347.1309	−6.6	$C_{15}H_{22}O_9$	329, 193	
61	9.09	Nepetalactone (Epi-nepetalactone)	165.0916	167.1074	3.8/4.5	$C_{10}H_{14}O_2$	147, 107/149, 121	But.
62	10.61	Dihydronepetalactone		169.1218	−2.9	$C_{10}H_{16}O_2$	151, 123, 83	
63	14.97	Kanokoside A	475.1817		1.6	$C_{21}H_{32}O_{12}$	339, 271	Rem. aq
64	15.80	Loganin		391.1634	8.9	$C_{17}H_{26}O_{10}$		
65	17.77	Patriscabroside I	361.1489		−1.1	$C_{16}H_{26}O_9$	196, 165	But., Rem. aq
66	21.56	Kanokoside C		639.2484	−1.7	$C_{27}H_{42}O_{17}$	621, 579, 562	
67	22.64	Deoxyloganic acid tetraacetate	527.1747		−2.3	$C_{24}H_{32}O_{13}$	459, 391, 323	But.
68	23.67	Kanokoside D		625.2671	−4.9	$C_{27}H_{44}O_{16}$	607, 581, 521	
		Mono and diterpenes						
69	13.33	Carnosic acid		333.2042	−5.4	$C_{20}H_{28}O_4$	315, 297	
70	13.53	Abienol		291.0687	−0.2	$C_{20}H_{34}O$	273, 217	
71	13.88	Carnosol		331.1913	2.7	$C_{20}H_{26}O_4$	278, 203	Rem. aq, MecH
72	17.08	Ethyl abietic acid		331.1690	−0.8	$C_{23}H_{22}O_2$	183	
73	18.28	12-*O*-Methylcarnosic acid	345.2070		2.9	$C_{21}H_{30}O_4$	299, 277	
74	18.93	Taxodione		315.1958	0.9	$C_{20}H_{26}O_3$	177, 123	
75	18.94	Coleonol (Forskolin)	409.2562		−5.5	$C_{22}H_{34}O_7$	351, 341	
76	19.01	Pachyphyllone	315.1958	317.2122	3.4	$C_{20}H_{28}O_3$	149	
77	19.60	Picrocrocin		331.1741	−3.2	$C_{16}H_{26}O_7$	183, 149	
78	21.03	Neoandrographolide		481.2781	−3.1	$C_{26}H_{40}O_8$	441, 401	
79	21.61	Abietic (Sylvic) acid		303.2223	−3.2	$C_{20}H_{30}O_2$	165	
80	22.85	Casearborin E		597.2730	2.8	$C_{33}H_{40}O_{10}$	579, 553	
81	23.82	Casearborin C/D		555.2575	−2.4	$C_{31}H_{38}O_9$	527	
82	24.25	Casearborin A		539.2663	4.4	$C_{31}H_{38}O_8$		EtOAc, But., Rem. aq
83	24.91	Dihydrotanshinone I		279.1027	4.2	$C_{18}H_{14}O_3$	149	MecH
		Triterpenes						
84	16.05	Corosolic acid		473.2323	0.1	$C_{30}H_{48}O_4$	455	MecH
85	17.22	Asiatic acid		489.3607	6.7	$C_{30}H_{48}O_5$	453, 407, 201	MecH, EtOAc
86	19.21	Ursolic acid methyl ester		471.3478	1.8	$C_{31}H_{50}O_3$	425, 407	
87	20.87	Melilotoside A		591.4307	8.2	$C_{35}H_{58}O_7$	574, 292, 133	
88	21.31	Platanic acid		459.3481	2.7	$C_{29}H_{46}O_4$	442, 316	But.
89	21.92	Orthosiphol D		553.2685	−0.7	$C_{31}H_{36}O_9$	525	
90	23.53	Unknown triterpene (Swietmanin I)		567.2609	3.6	$C_{32}H_{38}O_9$		
91	22.71	Micromeric acid		455.3526	1.3	$C_{30}H_{46}O_3$	437, 247, 203	
92	23.25	Ursolic acid		457.3684	1.6	$C_{30}H_{48}O_3$	439, 411, 393	
93	25.26	Conrauidienol		467.3876	−1.7	$C_{32}H_{50}O_2$	450	
		Fatty acids and esters						
94	7.83	Pinellic acid	329.2337		4.2	$C_{18}H_{34}O_5$	211, 171	MecH
95	14.89	16-Hydroxyhexadecanoic acid (Juniperic acid)	271.2267		−0.3	$C_{16}H_{32}O_3$	225	MecH
96	17.56	Myrestic acid	227.2007		0.6	$C_{14}H_{28}O_2$		Rem. aq
97	19.19	Palmitoleic acid	253.2173		4.3	$C_{16}H_{30}O_2$		
98	19.31	Hydroxyoctadecatrienoic acid		295.2268	−6.7	$C_{18}H_{30}O_3$	277, 179	
99	19.58	Linolenic acid	277.2182		−0.3	$C_{18}H_{30}O_2$		
100	22.73	Palmitic acid	255.2318		−0.1	$C_{16}H_{32}O_2$	237	
101	23.18	Tetracosanoic (Lignoceric) acid	367.3574		1.0	$C_{24}H_{48}O_2$		
102	23.46	Methyl 12,13-epoxystearate		313.2753	5.0	$C_{19}H_{36}O_3$	257, 239, 97	MecH, But.
103	23.52	Glyceryl palmitate		331.2858	4.7	$C_{19}H_{38}O_4$	239	
104	23.77	Oleic acid	281.2485		3.6	$C_{18}H_{34}O_2$		
105	25.55	Methyl oleate	295.2628		−1.1	$C_{19}H_{36}O_2$		
106	26.48	3-Hydroxypropyl oleate		341.3038	−3.6	$C_{21}H_{40}O_3$	95	
107	26.66	Eicosadienoic acid		309.2762	−8.2	$C_{20}H_{36}O_2$	291, 109	
Aliphatic and Hydroxybenzoic acid derivatives								
108	1.18	Tartaric acid	149.0098		−2.0	$C_4H_6O_6$		
109	1.21	Quinic acid	191.0549		−0.5	$C_7H_{12}O_6$	111	Rem. aq
110	1.35	3,4-Dihydroxyphenylacetic acid	167.0007		−0.9	$C_8H_8O_4$	148, 78	
111	1.37	2-Isopropylmalic acid	175.0588		8.6	$C_7H_{12}O_5$		But.
112	1.38	Galacturonic acid	193.0709		2.0	$C_6H_{10}O_7$		MecH
113	1.39	Malic acid	133.0500		−0.9	$C_4H_6O_5$		Rem. aq, But.
114	1.40	Protocatechuic acid hexoside	315.0716		1.8	$C_{13}H_{16}O_9$	195, 153, 109	But., Rem. aq
115	1.41	Hydroquinone glucuronide	285.0592		−4.5	$C_{12}H_{14}O_8$	165, 152	But.

Table 3. *Cont.*

Peak #	RT. (min.)	Metabolite Name	Mol. Ion *m/z*		Mass (ppm)	Elemental Composition	MS^2 Ions *m/z* (−)/(+)	Fractions
			$[M-H]^-$	$[M+H]^+$				
116	1.48	Hydroxyphenyllactic acid	181.0486		−5.0	$C_9H_9O_4$	166, 112	
117	4.57	Suberic acid	173.1190		0.1	$C_8H_{14}O_4$		
118	6.39	Tuberonic acid (12-hydroxy-7-isojasmonic acid)		227.1286	3.6	$C_{12}H_{18}O_4$	209, 191, 131	
119	6.61	Pinonic acid	183.1021		2.7	$C_{10}H_{16}O_3$	137	But.
120	16.93	Menthyl salicylate		277.1786	−4.3	$C_{17}H_{24}O_3$	231, 137	
		Others						
121	1.26	Valine		118.0862	−3.9	$C_5H_{11}NO_2$	58	
122	1.68	Niacin (nicotinic acid)		124.0393	1.0	$C_6H_5NO_2$	106, 80	
123	2.12	Proline		116.0706	−7.2	$C_5H_9NO_2$	84, 70	
124	4.25	Oleacein		321.1337	1.2	$C_{17}H_{20}O_6$	149	MecH, EtOAc, But.
125	4.34	Hydroxyquinoline		146.0600	−1.1	C_9H_7NO	118, 91	
126	8.05	Loliolide		197.1166	−3.3	$C_{11}H_{16}O_3$	179, 105	
127	10.58	Tryptophol		162.0913	5.8	$C_{10}H_11NO$	146, 118	
128	26.89	7-hydroxy-4-methyl-coumarin (Hymecromone)		177.0543	−1.6	$C_{10}H_8O_3$	159, 149	But.

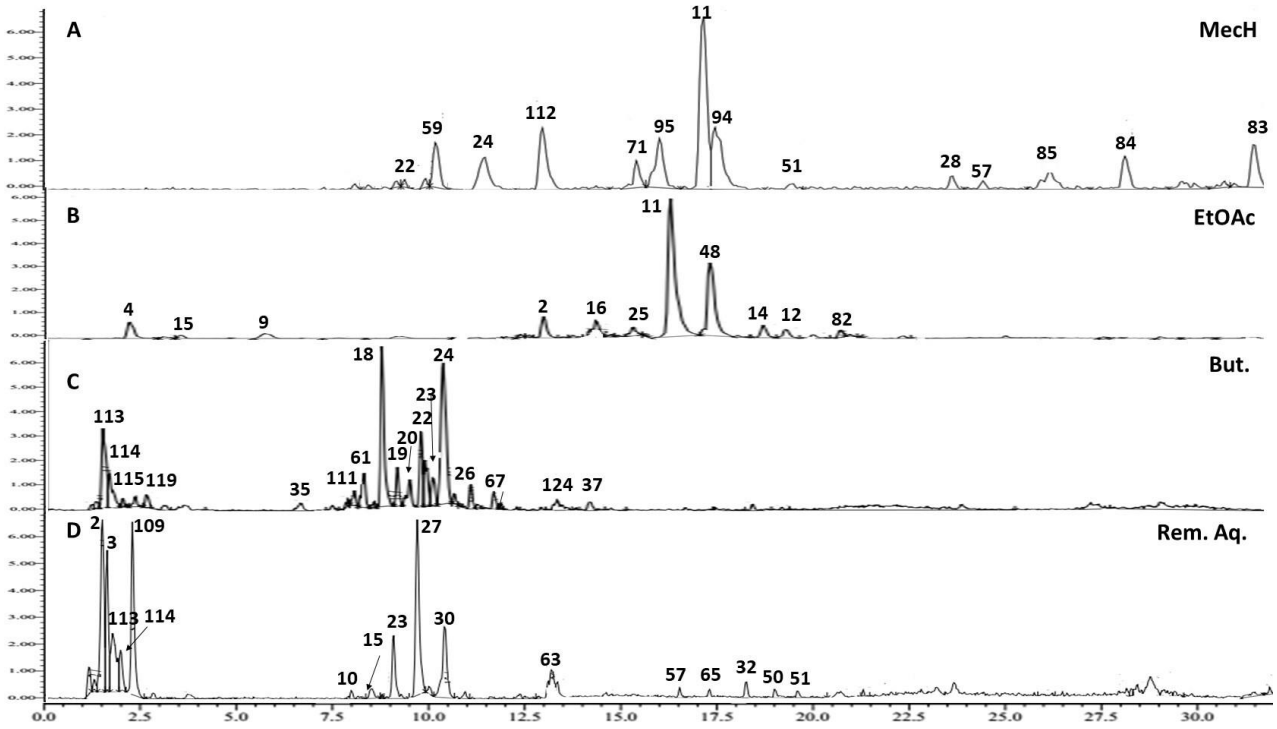

Figure 6. Representative UPLC/TOF-MS base peak chromatograms of fractions of *Mentha pulegium* L. (MP) in negative mode, (**A**) Methylene chloride fraction (MecH), (**B**) Ethyl acetate fraction (EtOAc), (**C**) Butanol fraction (But.) (**D**) Remaining aqueous fraction (Rem. Aq.). Peak numbers follow metabolites listed in Table 3.

2.3.1. Hydroxycinnamic Acids and Derivatives

Fourteen hydroxycinnamic acid conjugates were detectable in MP metabolite profile, half of which were eluted first and occupied the early section of the chromatogram at a retention time range (t_R) of 1.31–5.17 min. Caffeoyl-*O*-glucuronide assigned for peak 1 with molecular ion *m/z* 355.0852 $[M-H]^-$ (t_R = 1.31 min, and predicted chemical formula $[C_{15}H_{15}O_{10}]^-$), exhibited two daughter ions; *m/z* 193.0739 and *m/z* 161.0428 in MS^2 spectra, representative of glucuronyl and caffeoyl fragments, respectively (Figure S1). Sinapoyl-*O*-hexoside, ascribed for molecular ion *m/z* 387.1408 $[M+H]^+$ (peak 5, t_R = 1.87 min, $[C_{17}H_{23}O_{10}]^+$), generated a daughter ion; *m/z* 225.0784 with predicted chemical formula $[C_{11}H_{13}O_5]^+$, corresponding to a sinapoyl moiety and the mass difference of (162 amu) between the two ions signifies the loss of the hexose moiety (Figure S2). Caffeic acid

dimers and oligomers, termed "depsides" *viz.* salvianolic and rosmarinic acids, are discriminative phytochemical markers of family Lamiaceae [18]. Five caffeoyl dimer metabolites were tentatively identified in MP extract; peaks # 4, 8, 9, 10, and 11 as caffeic acid dimer, salvianolic acid K, caffeoyl-sinapoylquinic acid, salvianolic acid F and rosmarinic acid, respectively. Rosmarinic acid, the ester of 3,4-dihydroxyphenyllactic acid (danshensu, or salvianic acid A) and caffeic acid, was ascribed to molecular ion m/z 361.0907 $[M + H]^+$ (peak 11, t_R = 12.55 min, $[C_{18}H_{17}O_8]^+$), where the MS^2 examination showed a fragment at m/z 197.0104 ($[M + H - C_9H_{10}O_5]^+$) signifies the danshensu moiety, and the neutral loss of 164 amu signifies the caffeoyl group (Figure S3). Peak 8 at m/z 557.1252 $[M + H]^+$, (t_R = 7.26 min, $[C_{27}H_{25}O_{13}]^+$) gave fragments at m/z 511.0066 ($[M + H - CO_2]^+$) and 363.1261 ($[M + H - C_9H_6O_5]^+$, considered for the loss of carboxylic group and danshensu, respectively, and the compound was identified as salvianolic acid K (Figure S4). Salvianolic acid F, another depside of caffeic acid was annotated to the ion at m/z 315.0836 $[M + H]^+$ (peak 10, t_R = 8.98 min, $[C_{17}H_{15}O_6]^+$), revealed a fragment ion at m/z 181.0863 with the chemical formula $[C_9H_9O_4]^+$, signifying the caffeic acid moiety (Figure S5). Although other salvianolic acids have been reported in pennyroyal, to our knowledge, salvianolic acids K and F are reported herein for the first time in Egyptian MP, in addition to caffeoyl-sinapoylquinic acid (Figure S6).

2.3.2. Flavones and Derivatives

The flavonoid configuration of MP extract was dominated by 18 flavone compounds detected with varying abundances and eluted in the order of 10 flavone conjugates (t_R = 4.86–10.32 min). Followed by 8 flavone aglycones (t_R = 10.42–16.88 min) (Figure 5). Apigenin 6,8-di-*C*-hexoside (vicenin 2) was assigned to the ion detected at m/z 593.1489 $[M - H]^-$ (peak 15, t_R = 4.87 min, $[C_{27}H_{29}O_{15}]^-$) based on the fragment ions at m/z 353.0645, 383.0711 amu for $[Apg + 83/Apg + 113]^-$ typifying a di-*C*-glycoside of apigenin [19], (Figure S7). Vicenin 2 was reported in *Origanum* species of Lamiaceae, but not in pennyroyal [9].

Three glucuronide conjugates of penduletin, luteolin and apigenin were assigned to molecular ions at m/z 521.1812, 463.0899, and 447.0827 amu, peaks 16, 21, and 22, respectively (Figures S8–S10), where the MS^2 data showed the fragment ions respective to the aglycones at m/z 345.1507, 287.0550, and 271.0593 signifying the loss of a glucuronide moiety $[M + H - 176]^+$. The flavone glycoside diosmin (diosmetin 7-*O*-rutinoside), which has been repeatedly reported in several members of the genus Mentha [9] was ascribed to the ion at m/z 609.1782 $[M + H]^+$, (peak 20, t_R = 7.79 min, $[C_{28}H_{33}O_{15}]^+$) by the abundance of the daughter ions at m/z 463.1208 and 301.0695 amu, indicative of the cleavage of the deoxyhexose (146 amu) followed by the hexose moieties (162 amu), respectively (Figure S11). A molecular ion was observed with high abundance at m/z 327.2178 $[M - H]^-$ (peak 17, t_R = 7.15 min, $[C_{18}H_{15}O_6]^-$), was tentatively identified as the flavone salvigenin after generating a daughter peak at m/z 190.9540 amu denoting the deprotonated dimethoxy substituted moiety left after C-ring cleavage of the aglycone by Retro-Diels–Alder reactions (Figure S12) [20]. Similarly, acacetin was annotated to the molecular ion at m/z 285.0753 $[M.+; H.]^+$ (peak 29, t_R = 14.23 min, $[C_{16}H_{13}O_5]^+$), after the aglycone cleavage along C-ring to give the fragment ion at m/z 153.0169 amu (Figure S13). Acacetin-*O*-rutinoside (linarin) was readily assigned to the ion at m/z 593.1879 $[M + H]^+$ (peak 23, t_R = 9.35 min, $[C_{28}H_{33}O_{14}]^+$) which yielded the fragment ions at m/z 447.1286 after loss of the deoxyhexose (146 amu) followed by the fragment ions at m/z 285.0767 representing the aglycone after the loss of a hexose moieties (162 amu) (Figure S14).

2.3.3. Flavanones and Flavanol Derivatives

Seven flavanones and flavanol derivatives were detected in the 70% ethanol metabolite profile of pennyroyal. Naringenin-7-*O*-glucuronide was assigned to the molecular ion at m/z 449.1112 $[M + H]^+$ (peak 33, t_R = 5.07 min, $[C_{20}H_{21}O_{11}]^+$), whereas eriodictyol-7-*O*-glucuronide was assigned to the molecular ion at m/z 463.0990 $[M - H]^-$ (peak 36,

t_R = 8.16 min, $[C_{21}H_{19}O_{12}]^-$) by the observed ions in MS^2 spectra at m/z $[273.0965]^+$ and $[286.9356]^-$, respectively, implying the neutral loss of a 176 amu for the glucuronide moiety (Figures S15 and S16). A major peak (39), eluded at t_R = 21.51 min in the positive ionization mode, produced an intense molecular ion at m/z 611.2864 that exhibited a predicted chemical formula $[C_{28}H_{35}O_{15}]^+$. The metabolite was annotated hesperetin 7-*O*-rutinoside (hesperidin) as reported previously in pennyroyal [21] and confirmed by the fragment ion at m/z $[465.2265]^+$ implying the loss of a deoxyhexose portion (146 amu) (Figure S17).

2.3.4. Prenyl Flavanones

Mass spectrometry-based detection is a powerful tool for discovering minor secondary metabolites of potential medicinal merit in plant extracts [22]. The analytical procedure adopted in this study succeeded in tentative identification of seven prenylated flavones in MP extract for the first time. A molecular ion of low abundance at m/z 353.2329 $[M - H]^-$ (peak 41, t_R = 7.24 min, $[C_{20}H_{17}O_6]^-$) was assigned prenyl kaempferol after the neutral loss of 68 amu (isoprenyl group) to yield a fragment ion at *m/z* $[285.1418]^-$ with the predicted chemical formula of kaempferol $[C_{15}H_9O_6]^-$ (Figure S18). Similarly, another molecular ion of low abundance at m/z 339.216 $[M - H]^-$ (peak 45, t_R = 14.99 min, $[C_{20}H_{19}O_5]^-$) was annotated prenyl naringenin, generating the daughter ion at m/z $[271.2282]^-$ with the predicted chemical formula of naringenin $[C_{15}H_{11}O_5]^-$ after the loss of 68 amu (Figure S19).

2.3.5. Biflavanoids

Amentoflavone has been reported previously in horse mint (*Mentha longifolia*) [23] and sweet marjoram (*Origanum majorana*) [24] of family Lamiaceae. In this study, five biflavonoids have been tentatively identified in the metabolome profile of MP for the first time. Di-*O*-methylamentoflavone (ginkgetin) was assigned to the molecular ion at m/z 567.1288 $[M + H]^+$ (peak 50, t_R = 18.88 min, $[C_{32}H_{23}O_{10}]^+$) which gave in MS^2 spectra a base peak at m/z $[297.0760]^+$ typifying the di-*O*-methyl-apigenin monomer of the biflavonoid molecule, and a fragment ion at m/z $[165.0206]^+$ after further cleavage along its C-ring (Figure S20). The methyl derivative of ginkgetin, sciadopitysin (amentoflavone-7,4′,4‴-trimethyl ether), was allocated to the molecular ion at m/z 581.1424 $[M + H]^+$ (peak 51, t_R = 21.59 min, $[C_{33}H_{25}O_{10}]^+$) after generating the same base peak at m/z $[297.0760]^+$ in MS^2 spectra (Figure S21).

2.3.6. Terpenes

Members of the Lamiaceae are known to accumulate a wide variety of mono, diterpenes, or even triterpenes of significant medicinal and industrial value. The Dictionary of Natural Products listed more than 2000 diterpene constituents in family Lamiaceae [25]. Labdane core diterpenes feature Lamiaceae characteristic marker metabolites and in accordance, abienol (peak 70, t_R = 13.53 min, m/z 291.0687 $[M + H]^+$, $[C_{20}H_{35}O]^+$) and coleonol (peak 75, t_R = 18.94 min, m/z 409.2562 $[M - H]^-$, $[C_{22}H_{33}O_7]^-$) were tentatively identified in MP profile (Figures S22 and S23). The phenolic diterpenes, carnosic acid (peak 69, t_R = 13.33 min, m/z 333.2042 $[M + H]^+$, $[C_{20}H_{29}O_4]^+$), and carnosol (peak 71, t_R = 13.88 min, m/z 331.1913 $[M + H]^+$, $[C_{20}H_{27}O_4]^+$) are known active secondary metabolites which have been reported in rosemary (Lamiaceae) [26] (Figures S24 and S25). Two abietane diterpenoids, pachyphyllone (peak 76, t_R = 19.01 min, m/z 317.2122 $[M + H]^+$, $[C_{20}H_{29}O_3]^+$) had a fragmentation pattern matching that reported in [27] (Figure S26), in addition to dihydrotanshinone I, (peak 83, t_R = 24.91 min, m/z 279.1027 $[M + H]^+$, $[C_{18}H_{15}O_3]^+$) another characteristic diterpenes of Lamiaceae characterized by a base peak at m/z $[149.0241]^+$, for benzofuran-4,5-dione in MS^2 spectra [28] (Figure S27). Asiatic acid (peak 85, t_R = 17.22 min., m/z 489.3607 $[M + H]^+$, $[C_{30}H_{48}O_5]^+$) exhibited a fragmentation pattern matching that reported in [29] (Figure S28). Ursolic acid (peak 92, t_R = 23.25 min., m/z 457.3684 $[M + H]^+$, $[C_{30}H_{48}O_3]^+$) was assigned after generating fragmentation ions in MS2 spectra at m/z $[439.3539]^+$ and $[411.3628]^+$ for dehydration and decarboxylation of the parent ion, respectively. According to the data, the fragmentation ions at m/z $[203.1787]^+$

and [191.1794]$^+$ are Retro-Diels-Alder reaction products for Δ 12-unsaturated pentacyclic triterpenes [30] (Figure S29).

3. Discussion

Pregnant women usually turn to self-medication, relying on herbal and natural products to relieve pregnancy related ailments, or even for pregnancy termination, regardless of the lack of evidence concerning the safety profile of these products. This study targets the biological, behavioral, pathological, and toxicological consequences prior to administering the 70% ethanol extract of *Mentha pulegium* L. (MP) in pregnant female rats. This aim was executed over two parts; the first part includes probing the abortifacient potential using different doses of MP 70% ethanol extract to specify the effective abortifacient dose. Designating the abortifacient effect will rely on assessing some parameters, including percentage of abortion per group, number of resorbed fetuses, and further correlation to serum progesterone levels for confirmation of the results. On the 18th day of gestation, animals were sacrificed, and the uteri were examined. After specifying the dose of 250 mg/kg of MP extract as an abortifacient dose comparable to the standard misoprostol, the study attempts, in the second part, to unravel the mechanistic pathway underlying the abortifacient action. Additionally, the fractions of the 70% ethanol extract of MP, prepared as described in Section 5.1, were also similarly examined to trace the phytochemical constituents responsible for this effect.

Maternal exposure to MP (extract and/or fractions thereof) and misoprostol resulted in teratogenic anomalies represented by the asymmetrical distribution of fetuses in both uterine horns, resorption sites, intensive bleeding, complete absence of fetus on one uterine horn, absence of boundaries between fetal balls, and small fetal balls. Additionally, their fetuses suffered from IUGR, morphologic malformations, hematoma, transparency of skin, and intensive bleeding. In line with our findings, a previous documentation of teratogenicity and reproductive toxicity signs induced in pregnant rats exposed to pesticides on uterus and fetus investigation [31]. As a reinforcement to our data, unsuccessful use of misoprostol as an abortifacient was associated with preterm delivery, uterine rupture, and congenital malformations [15,16].

Estrogen and progesterone are cornerstones of healthy successful gestation with normal fetal growth [32]. Both hormones increase throughout pregnancy compared to unpregnant states, followed by a sharp decline in progesterone levels towards the end of gestation for labor induction [33]. Affecting these steroidal hormone trajectories, such as their production, transport, and receptors, may result in abortion (intended) or miscarriage (unintended), and IUGR [34,35]. In the current work, treatments with MP extract and misoprostol significantly affected serum sex hormones, which may be a reason for the complete abortion or fetal resorption observed in treated rats. In agreement with a previous study that demonstrated misoprostol power to modulate serum level of estrogen and progesterone to induce abortion, and misoprostol-mediated structural abnormalities in survival fetus [14]. Furthermore, all the fractions showed an anti-progesterone effect, whereas But. and the Rem.aq. exhibited additional definite estrogenic activities. This fluctuation in sex hormone levels were manifested by the obvious growth resistance and the increased fetal resorption that was documented in their groups. The findings reported herein imply that a possible abortifacient effect of MP is to decrease progesterone levels and increase estradiol levels.

MicroRNAs (MiRs) are non-coding small molecules known as "fine-tuners" rather than "switches" as they balance gene expression in the posttranscriptional state [36,37]. Nowadays, MiRs are gaining significant attention and became a field of study by researchers targeting its implication in the disease progression and maintaining tissue homeostasis. On the other side, MiRs titers during normal pregnancy or disorder states, such as abortion, preterm labor, pre-eclampsia, IUGR, and congenital deformity did not receive the same recognition. Hence, investigating them will aid in establishing new therapeutic and diagnostic targets in pregnancy related complications. A single change in miRNA expression,

at any stage of placental or fetal development, can lead to serious complications which was observed herein. All the treated rats exhibited disrupted MiRs expression that may be one of the contributing factors to IUGR, fetal resorption, and even complete abortion. The administration of Rem.aq was associated with the highest up regulation in MiR-520 among fractions that sequentially resulted in additional toxicity observed in its group. Previous studies documented that MiR-520 upregulation in both placenta and maternal circulation is highly linked to placental pathologies, such as IUGR [38] and our records of declined fetal weight supports this fact. Concerning MiR-146a, its up-regulation is highly associated with balanced micro-environment of pregnancy, and its downregulation was involved in unexplained spontaneous abortion [39] in agreement with our data.

Substances that mimic or stimulate different MiR-520 isoforms regulate and increase estradiol [40] and that is concurrent with our findings where misoprostol, MP extract, and its fractions upregulated MiR-520 that, in turn, increased estradiol (Figure 3II), resulting in abortion or IUGR. Concerning miRNAs-146, formerly it was documented that mature miRNAs-146 in endometrial epithelial cells are upregulated by progesterone that, in turn, will antagonize estrogen in endometrial epithelium [41], all these facts were reverted by MP (extract and fraction) and misoprostol administration to induce IUGR, fetal morphological deformity, or even complete abortion, where MP; total extract and or its fractions, and misoprostol decreased progesterone that resulted in MiR-146a down-regulation resulting in inhibition of the posttranscriptional regulation of estradiol and increasing its levels.

Matrix metalloproteinases (MMPs) are the most important among the classes of proteolytic enzyme in matrix degradation with similar structures and variety of functions [42]. MMPs show elevated levels during normal pregnancy, as a part of essential regulation of vascular and uterine remodeling, since significant changes in the hemodynamic and uterus is required to allow adequate uteroplacental blood flow and uterine expansion for appropriate fetal growth [43]. MMP-9 upregulation has been implicated in placentation, vasodilation, and uterine expansion during normal pregnancy. Hence, our investigation probed MMPs expression and its regulator, the tissue inhibitors of metalloproteinases (TIMPs), where MMPs are inactivated through TIMPs [43], that is produced by the same cells that produce MMP-9. In this study, all the pregnant rats treated with misoprostol, MP (250 mg/kg) extract, and fractions thereof at a dose of 125 mg/kg, demonstrated a marked inhibition in MMP-9 protein expression because of upregulation of its inhibitor the TIMP-1 protein expression. Previous studies reported the decreased MMP-9 levels may be involved in the IUGR pathogenesis during pregnancy [44], and that was evident in this work where all the fetuses showed retarded growth expressed in reduced fetal weights comparable to fetuses of untreated mothers. Moreover, MMP-9 levels are affected by pregnancy hormones (progesterone and estradiol) [45] as it was depicted formerly that progesterone regulates MMP expression/activity, which helps in management of the initiation, maintenance, and progression of endometrium [46]. Hence, the MP associated disturbance in both hormones may be the reason behind the elevated TIMP-1 and the decrease in MMP-9 uterine expression.

A certain amount of inflammatory response is paramount to normal healthy gestation, however, its exaggeration by the imbalance between pro-inflammatory (TNF-α, IL-6, and IL-8) and anti-inflammatory (IL-10, and IL-4) cytokines/chemokines, and the stimulation of different signaling molecules may sequel in many complications, such as preterm labor, IUGR, and spontaneous abortion, which may even increase the risk of morbidity and mortality to both the mother and their offspring [47,48]. Furthermore, increasing maternal inflammation through periods of fetal development is considered as a significant risk factor for birth deficits, morphological deformity, congenital diseases, and even still birth [49,50]. In our study, a marked inflammatory state in both, misoprostol and MP treated rats was manifested by elevation in the levels of TNF-α and IL-1β which participates in the observed fetal deformity in different groups, in agreement with previously published data [51]. Notably, the cytokine IL-1β was the first parameter to be linked to infection-

induced premature labor. In addition, preterm labor and delivery were induced by IL-1β administration in experimental animals [52].

Phytochemical constituents in MP possess potential modulation of circulatory maternal hormones may trigger the inflammatory response as progesterone hinders the inflammatory related markers and molecules and keep the gestation environment protected [53]. Furthermore, the exaggerated inflammatory response observed herein after MP administration rationaled the disturbance in MMP-9/TIMP-1 expressions in their relevant treated groups (extract and fractions). Supporting this hypothesis, a previous study documented that overexpression of TNF-α, reduce MMP-2 and MMP-9, while an aggravation of the severity of abortion in rats further prompted TNF-α expression that sequentially decreased MMP-2 and MMP-9 levels [54]. In addition, using anti-inflammatory medication such as lactoferrin was able to prevent miscarriage/abortion by modulating MMP-9/TIMP-1 ratio and promoting repair [55]. Collectively, MP shifted the inflammatory state toward stimulation that increased risk of abortion or fetal resorption, IUGR, and morphological deformity.

Mood disorders *viz* depression and anxiety, addiction, and attempted suicide are mental health problems associated with abortion and placental pathologies induced by either stress or drugs [56]. Hence, brain investigations in this milieu have preoccupied researchers, and still there is no definite explanation available for its incidence nor prevention [57–59]. In this study, an open field test (OFT) was employed to examine the mental and behavioral status of the pregnant female rats under investigation. OFT is a widely used method of assessing rodent exploratory behavior, anxiety-like behaviors and determining whether a substance is sedative, poisonous, or stimulating. Consequently, the OFT assesses a variety of behavioral characteristics in addition to locomotion [60–63].

Taking into consideration all the analyzed parameters in OFT, only EtOAc and Rem.aq. treatment showed contrast behavioral effects, EtOAc treated rats showed depressive behaviors whereas Rem.aq. treated ones presented a state of anxiety and stress. Additionally, misoprostol treated group showed similar behavior to EtOAc treated group, even more pronounced. Several studies agree with the records of OFT variables and our interpretation [64–66]. In addition, this variance in behavior outcome, depression and/or anxiety, is common following early pregnancy loss or termination [67].

Glial fibrillary acidic protein (GFAP), is a major intermediate filament protein of differentiated astrocytes that plays a fundamental role in brain activity, not only in pregnancy but also physiologically as it modulates astrocytic motility and shape by supplying structural stability to astrocytic processes [68]. A previous study monitoring the changes in GFAP expression in the brain of rats during pregnancy and the beginning of lactation reported that GFAP expression is markedly increased on days 18 and 21 of gestation and is a sequence to changes in circulating sex steroid hormones. In the current study, administration of MP extract and its fraction on day 15th of gestation maintained GFAP cortical content on day 18th, except for Rem.aq., which showed a reduced GFAP content. Misoprostol treated rats presented the worst GFAP contents, implying a higher hazard/deleterious potential and this is the first documentation of this effect according to the author knowledge. Misoprostol and Rem.aq. changes in sex steroid hormones distinctly decreased GFAP cortical contents. Further, the decreased levels of GFAP may be in charge of the behavioral disturbance observed in rats treated with them [69].

Placental pathologies, mediated by altered MiRs levels, target gene expression of various signaling molecules that are important not only for fetal neurodevelopment but also for maintaining a normal maternal brain environment [70]. MiRs and other secreted compounds from the preeclamptic placenta showed direct effects on neurons and astrocytes [70], accordingly the changes of GFAP contents, may be related to misoprostol and Rem.aq. higher potential to modulate MicroRNAs.

Brain-derived neurotrophic factor (BDNF) is member of nerve growth factor family that has a structural role in neuronal development and function that is closely related to mood and behavioral disorders in many conditions [71]. All the treatments, except for But.,

decreased cortical contents of BDNF as compared to those of positive control reflecting neurogenesis inhibition. The reason behind this reduction may be the disturbance in hormonal status caused by both medical or herbal treatments for abortion induction [72,73]. Additionally, the decline in the cortical contents of BDNF contributes to the disruption in the behavior of pregnant rats as evidenced by OFT behavioral records after the different treatments. This was reinforced previously that the decline in BNDF levels have been linked to faster cognitive decline, poor memory performance, learning ability and even anxiety related behavior [62].

Serotonin, or 5-Hydroxytryptamine (5-HT) is the most manipulated monoamine for its role as a neurotransmitter in experimental animal models to establish its role in humans physiologically and pathologically. Misoprostol, MP extract and only EtOAc fraction increased cortical content of 5-HT, but the rest of the fractions did not affect brain 5-HT levels. Toxic placental effects perceived by these groups may also have a role in this monoamine increase. Our findings are supported by the theory which states that maternal mood and behavior are controlled by the placenta and that exposure to stressors or pathological conditions may result in an increase in 5-HT [74]. Additionally, altered serum progesterone and estradiol levels marked herein, participated in the increased 5-HT cortical content. As the regulation and modulation of neuronal excitability and neurotransmitter systems (5-HT is a one member of this system) is under the control of neurosteroids, steroid hormones with activity in the nervous system [75].

During the last century, the estrogenic properties of certain plants were recognized, initially in grazing animals, following the ingestion of clover revealed to contain high levels of the isoflavone compounds; formononetin and biochanin A [76]. Ever since, the term phytoestrogens have been established, referring to polyphenolic, non-steroidal plant constituents exerting estrogen-like biological action. Increasing epidemiological and chemical investigations pinpointed phytochemical classes viz. isoflavones, stilbenes, lignans, terpenes, and certain saponins as phytoestrogen candidates [77]. Phytoestrogens intake can modulate the endocrine system either by acting as agonists/antagonists for the estrogen receptors or by interfering with the estrogen biosynthesis process [78]. Apart from the estradiol-activating pathway, phytoestrogens can also exhibit their effects through non-genomic mechanisms, via interactions with cell surface receptors or by epigenetic mechanisms [41].

Like other members of the mint family, administration of *Mentha pulegium* L. extract and oil are known to pose fluctuations in estrogenic/progesterone levels and are used for terminating pregnancy [78,79]. The metabolic profile of MP extract reported herein in the results Section 2.3, encompasses a plethora of phytochemical constituents that were reported to possess effects on sex hormones.

Caffeic acid conjugates and depsides are the major water-soluble components detected in MP extract using UPLC-ESI-MS-TOF. A wide variety of pharmacological activities of these bioactive compounds have been evaluated including modulation of estrogen receptors [80,81]. Rosmarinic acid, a caffeic acid depside synthesized ubiquitously in the Lamiceae family and regarded as a marker, was reported to increase serum estradiol contents in diabetic and estrogen-deficient rats [82,83].

The metabolite profile of MP extract revealed the abundance of the flavone apigenin and several of its conjugates in addition to amentoflavone, which are reported in pennyroyal for the first time. Amentoflavone, a biflavonoid composed of two apigenin molecules, as well as its derivatives, were reported to be estrogen receptor agonists and inhibitors of aromatase enzymes in various experimental models [84,85]. A major metabolite of MP profile also was the flavone compound acacetin, which was proclaimed to be estrogen receptors agonists promoting uterine weight gain in mice [86]. Isoflavones are the most extensively studied compounds with established phytoestrogen activities [87], are represented in MP profile by a single constituent viz. daidzein-hexoside, enriched in the But. and Rem.aq. fractions. Daidzein was recorded to inhibit progesterone secretion, decrease the mRNA expression of α and β- estrogen receptors in medium ovarian follicles

of pigs [88]. Prenylated flavonoids are bioactive metabolites that possess a prenyl (isoprene) group attached to the flavane nucleus identified in about 37 genera of plant families *viz*. Leguminosae, Rutaceae, Guttiferae, and Apiaceae [89]. Prenylated flavonoids are mainly regarded as phytoalexins produced in response to pathogenic microorganism offense [90] and were identified in MP profile herein for the first time owing to the high sensitivity offered by the mass detection. These biometabolites are regarded as potent phytoestrogens with 8-Prenylnaringenin capacity to compete with 17 β-estradiol for estrogen receptors binding at a dose of 10 μM [89]. Although the analytical procedure adopted herein is not enough to assign the prenylation position, it is worth mentioning that the substitution at C8 is crucial for the activity, and 6-prenylnaringenin was proven to exert a much lower estrogenic activity than the 8-prenylated isomer [91].

Quinones are another group of metabolites reported previously in Salvia miltiorrhiza [92], and detected in MP extract and its fractions (Table 3) for the first time in this study. Tanshinone IIA, a reported potent phytoestrogen with active conformation analogous to 17 β-estradiol and high binding affinity to estrogen receptors, was detected in the 70% ethanol extract of MP, MecH and Rem. aq. fractions [93].

It is worth mentioning that all MP fractions imposed fetal morphologic malformations, if not complete abortion. In brief, all the fractions presented a significant reduction in fetal weight especially with the But. and rem. Aq. fractions in addition to the highest intrauterine growth retardation (IUGR). Both fractions also caused elevation in the levels of estradiol with a decline in serum progesterone levels as compared to healthy pregnant ones and those treated with MP extract. The rem. Aq. fraction showed the highest increase in MiR-520 and TNF-α values, compared to MP, whereas MecH fraction exhibited the highest effect on TIMP-1 and MMP-9 expressions. EtOAc treated rats showed depressive behaviors contrarily to Rem. aq. treated ones which demonstrated a state of anxiety and stress. Misoprostol treated groups showed similar, or even more pronounced behavioral state to EtOAc treated group. MP extract and its fractions caused a reduced GFAP content, and misoprostol resulted in the least GFAP contents. Misoprostol, MP extract, and EtOAc fraction increased cortical content of 5-HT. All the treatments, except for the But. fraction, decreased the cortical contents of BDNF as compared to those of positive control reflecting neurogenesis inhibition.

4. Conclusions

The data of the current study verifies and documents the traditional reputation of employing *Mentha pulegium* L. (Pennyroyal) as an abortifacient by modulating pregnancy hormone levels, gene/protein expression, and the inflammatory process. All these cues afflicted the fetal morphology and the mothers' brains and behavior. Indeed, MP was successful in terminating pregnancy with minimal behavioral abnormalities and low toxicity margin, yet contrarily to misoprostol, MP extract in the dose of 250 mg/kg maintained cortical contents of GFAP. UPLC-ESI-TOF-MS examination revealed MP and its fractions to encompass several metabolites with phytoestrogenic potential and mediating for the abortifacient effect. The findings reported herein encourage the future perspective of possible use of MP extract in contraception if administered at an earlier phase of the estrous cycle. Major phytochemical constituents identified in this study *viz.* rosmarinic acid, hesperidin and ursolic acid can be examined for their individual effects following the same presented model. The workflow reported in this study can be employed to investigate the safety profile of other edible or medicinal plants, particularly the herbs of family Lamiaceae, which are commonly consumed during pregnancy.

5. Materials and Methods

5.1. Plant Material

Aerial parts of *Mentha pulegium* L. (pennyroyal) were collected from El-Beheira Governorate in May, after blooming of the flowers. The taxonomic authentication was confirmed by Dr. Abdel Halem Abdel El Mogali, Professor in flora and phytotaxonomy research,

Agricultural Research Centre, where a voucher specimen No. (M.P. 998) is kept. Pennyroyal was dried in the shade then pulverized, and 200 g of the powdered plant was prepared by maceration in 70% ethanol. The extract was concentrated on a rotary evaporator (Buchi R-210 evaporator, Flawil, Switzerland) until completely dry, yielding 45 g for biological investigations and UPLC-ESI-TOF-MS analyses. Portion of AE (25 g) was reconstituted in water and partitioned with increasing polarity organic solvents, as methylene chloride (MecH), ethyl acetate (EtOAc), and butanol (But). Each organic fraction was carefully evaporated until completely dry, and the remaining liquor (Rem. aq.) was also concentrated under vacuum and freeze dried for UPLC-ESI-TOF-MS examination. Dried fractions were freshly dissolved in distilled water by sonication and 2 drops of tween 80 if needed before oral administration to the rats.

5.2. Chemicals and Reagents

Thermo-Fisher Scientific Co. (Waltham, MA, USA) supplied the solvents acetonitrile and methanol (HPLC grade), while Sigma–Aldrich Co. (St. Louis, MO, USA) supplied the mobile phase solvents ammonium hydroxide, formic acid 98 %, and misoprostol standard drug. Analytical grade solvents (methylene chloride, ethyl acetate, and butanol) used in preparing the fractions were also purchased from Sigma-Aldrich Company.

5.3. Experimental Design

5.3.1. Part I: Dose Selection

A dose range-finding study was conducted to screen and select the optimal abortive dose of MP extract using 48 mature albino rats, comprised of40 females (180–200 g) and 8 males (230–250 g) [94] purchased from the National Research Centre, Giza, Egypt and housed in clean plastic cages open to the room environment temperature of 24 ± 1 °C, humidity (55 ± 5%), exposed to 12 h light/dark cycle, and allowed free access to food and water throughout the study. The study was approved by Misr University for Science and Technology's institutional ethics committee for the use of laboratory animals with approval No. PT13 on 6 March 2021 and was supervised by the Guide for the Care and Use of Laboratory Animals (NIH publication, 1996).

After acclimation for one week, mating was ordered in a 1:5 ratio, where one male rat was introduced into five caged fertile female rats overnight [95]. Mating was confirmed on the next day in the early morning by carefully inserting a cotton-tipped swap moistened with normal saline into the vaginal cavity, then withdrawing after gently rolling it against the vaginal wall [14,96]. Successful mating is marked by the presence of vaginal plugs, positive animals were considered pregnant, and this day was considered as their first day of gestation [97–99]. Pregnant females were also confirmed by non-invasive techniques as monitoring the physical appearance of the enlarged abdomen and eventually the noticeable body mass increase [95,100]. Hence, we used six additional un-mated female rats as a negative control to compare changes in weight through the experiment, and two of them were sacrificed at the end of the experiment, and their uteruses were preserved in formalin for histopathological examination.

On the 15th day of gestation, female rats with confirmed pregnancies were randomly divided into five groups as follows: Group I: pregnant rats serving as positive control group. Group II: rats were treated by misoprostol (100 ug/kg; once per day orally for three days) to induce abortion and served as standard control group. This dose was selected after a pilot study (data not included), guided by previous studies used misoprostol alone in abortion induction [14,101]. Group III, IV, and V received 125, 250, and 500 mg/kg of MP extract, respectively (once per day for three days starting on day 15th). The number of the completely aborted rats per group, abortion percent were calculated, the number of fetuses remaining were counted, and serum progesterone was leveled. These parameters along with the histopathological examination (n = 2/per group) were used for the assessment of the optimal abortion dose of different doses of MP extract.

5.3.2. Part II: Identification of the Abortifacient Mechanism of MP Extract and Fractions Thereof

In this part, the sample size of male rats was increased as a conclusion from the different performed trials in the dose selection part where mating ratio 1:5 was associated with higher pregnancy failure and time consuming. Consequently, 20 male rats were randomly used for the mating of 42 female rats with a ratio 1:1 with the same previously described procedures of pregnancy confirmation in the previous section (dose selection). After the verification, the positive female rats were randomly allocated as follows: Group I: pregnant female rats that is served as positive control; Group II: rats in this group received misoprostol (100 ug/kg, orally) on day 15th of gestation; Group III: received the optimal dose of MP extract selected according to the results perceived from the first part of the study; 250 mg/kg once per day for three consecutive days starting on day 15 till day 17; Groups IV, V, VI, and VII received different fractions of MP orally (125 mg/kg; MecH, EtOAc, But., and Rem. Aq., respectively).

5.4. Tissue and Serum Preparation

On the 18th day of gestation, all animals' blood samples were collected via the retro-orbital sinus under anesthesia, followed by scarification by cervical dislocation, then decapitated. The uterus, placenta, and brain cortex were rapidly removed and washed with saline. The fetuses were isolated from the uterus of different groups to screen for the changes in weight and morphology to healthy ones correspondingly.

5.5. Behavioral Open Field Test (OFT)

The test was commenced 24 h after the last treatment. The apparatus matches the specifications described by previous studies [102,103]. Each rat was placed individually in the center of the apparatus to be tested, the apparatus was cleaned with 70% ethanol and allowed to dry prior to each individual trial. A video camera was placed in the center of the arena above the apparatus to record the experiment for the subsequent analysis of (i) latency time (time spent from placing the animal into the center of the device till its first move), (ii) ambulation frequency (number of squares crossed by the animal over 3 min.), (iii) rearing frequency (number of times the animal stood extended and extended on rear appendages with no forelimb support), and (iv) grooming frequency (number of times of rapid cleaning movements of the forelegs towards the face and/or the body (licking the fur, washing the face, or scratching behavior) as guided by a previous study [104].

5.6. Parameters Assessed by ELISA Technique

As mentioned in Appendix A.

5.7. Histopathological Examinations

As mentioned in Appendix B.

5.8. Quantitative Real-Time PCR for miR-520 and miR146a Placental Expression

As mentioned in Appendix C.

5.9. Western Blotting

As mentioned in Appendix D.

5.10. Statistical Analysis

GraphPad Prism software (version 5.0d; GraphPad Software, Inc., San Diego, CA, USA) was used for all statistical analyses. The data were articulated using analysis of variance (ANOVA), followed by Tukey's post hoc test. A Two-Way Repeated Measures (RM) ANOVA with one factor repetition (time: day) was employed to analyze the change in rat weight. The non-parametric data were expressed as the median (min–max) and were analyzed using the non-parametric Kruskal–Wallis followed by Dunn's as the post hoc test.

All the values were expressed as the mean of six rats ± S.D.A and the difference at $p < 0.05$ was considered statistically significant.

5.11. Metabolite Profiling of Pennyroyal (MP) Extract and Active Fractions by UPLC-ESI-TOF-MS

5.11.1. Sample Preparation

Stock solutions of pennyroyal (MP) extract and the active fractions (MecH, EtOAc, But., and Rem. Aq.), were prepared by separately dissolving 50 mg of each extract in 1 ml of the solvent mixture (Water: Methanol: Acetonitrile, 50:25:25 *v*/*v*). The samples were vortexed for 2 min, ultrasonicated for 10 min, and centrifuged at 10,000 rpm for 5 min, to obtain a final concentration of 2.5 µg/µL and 10 µL of the prepared solution was injected. The LC-MS analysis procedure was also used for blank samples, quality control samples, and internal standards used for experiment setup validation. Instrument setup, spectral acquisition, and MS-data processing were adjusted as mentioned in [105,106], and provided in the Supplementary Materials. Mass spectral data of identified metabolites in both ionization modes were compared to available online libraries and databases, *viz.* Human Metabolome Database and Pubchem. In addition, retention times and fragmentation patterns were compared to available reference standards.

5.11.2. Instrument and Spectral Acquisition

As mentioned in Appendix E.

Supplementary Materials: The following supporting information can be downloaded at: https://www.mdpi.com/article/10.3390/toxins14050347/s1, Figure S1: ESI-MS/MS Spectrum of peak (1) in the negative ion mode; Figure S2: ESI-MS/MS Spectrum of peak (5) in the positive ion mode; Figure S3: ESI-MS/MS Spectrum of peak (11) in the positive ion mode; Figure S4: ESI-MS/MS Spectrum of peak (8) in the positive ion mode; Figure S5: ESI-MS/MS Spectrum of peak (10) in the positive ion mode; Figure S6: ESI-MS/MS Spectrum of peak (9) in the negative ion mode; Figure S7: ESI-MS/MS Spectrum of peak (15) in the negative ion mode; Figure S8: ESI-MS/MS Spectrum of peak (16) in the positive ion mode; Figure S9: ESI-MS/MS Spectrum of peak (21) in the positive ion mode; Figure S10: ESI-MS/MS Spectrum of peak (22) in the positive ion mode; Figure S11: ESI-MS/MS Spectrum of peak (20) in the positive ion mode; Figure S12: ESI-MS/MS Spectrum of peak (17) in the negative ion mode; Figure S13: ESI-MS/MS Spectrum of peak (29) in the positive ion mode; Figure S14: ESI-MS/MS Spectrum of peak (23) in the positive ion mode; Figure S15: ESI-MS/MS Spectrum of peak (33) in the positive ion mode; Figure S16: ESI-MS/MS Spectrum of peak (36) in the negative ion mode; Figure S17: ESI-MS/MS Spectrum of peak (39) in the positive ion mode; Figure S18: ESI-MS/MS Spectrum of peak (41) in the negative ion mode; Figure S19: ESI-MS/MS Spectrum of peak (45) in the negative ion mode; Figure S20: ESI-MS/MS Spectrum of peak (50) in the positive ion mode; Figure S21: ESI-MS/MS Spectrum of peak (51) in the positive ion mode; Figure S22: ESI-MS/MS Spectrum of peak (70) in the positive ion mode; Figure S23: ESI-MS/MS Spectrum of peak (75) in the negative ion mode; Figure S24: ESI-MS/MS Spectrum of peak (69) in the positive ion mode; Figure S25: ESI-MS/MS Spectrum of peak (71) in the positive ion mode; Figure S26: ESI-MS/MS Spectrum of peak (76) in the positive ion mode; Figure S27: ESI-MS/MS Spectrum of peak (83) in the positive ion mode; Figure S28: ESI-MS/MS Spectrum of peak (85) in the positive ion mode; Figure S29: ESI-MS/MS Spectrum of peak (92) in the positive ion mode; Table S1: The PCR primers used for quantitative PCR analysis

Author Contributions: D.M.R.; Conceptualization, D.M.R., A.A.E.-G., G.M.R. and A.M.E.; Investigation, Methodology, resources, data curation, supervision and formal analysis, A.A.E.-G. and G.M.R. conducted the in vivo experiments, D.M.R. and A.M.E. UPLC/MS data interpretation, D.M.R. and A.A.E.-G. Writing—original draft preparation. All authors have read and agreed to the published version of the manuscript.

Funding: The research was self-funded.

Institutional Review Board Statement: Not applicable.

Informed Consent Statement: Not applicable.

Data Availability Statement: Data are available upon request from the corresponding author (daliarasheed@o6u.edu.eg).

Acknowledgments: Authors would like to acknowledge Mohamed Rasheed for procuring the plant material and extend their appreciation to staff of "The Proteomics and Metabolomics Unit" (https://www.57357.org/en/department/proteomics-unit-dept/about-department/), at the Children Cancer Hospital (CCHE-57357), for their tenacious efforts in empowering research in Egypt.

Conflicts of Interest: The authors declare no conflict of interest.

Abbreviations

BDNF	brain derived neurotrophic factor
But	butanol
EtOAc	ethyl acetate
GFAP	glial fibrillary acidic protein
5-HT	seretonin
IL-1β	interlukin-1 beta
IUGR	intra-uterine growth retardation
MecH	methylene chloride
MiR-146a	micro-RNA 146a
MiR-520	micro-RNA 520
MMP-9	matrix metalloproteinase-9
MP	Mentha pulegium
OFT	open field test
Rem. aq	remaining aqueous liquor
TIMP-1	tissue inhibitor matrix metalloproteinase-1
TNF-α	tumor necrosis factor-alfa
UPLC-ESI-TOF-MS	ultra performance liquid chromatography-electrospray ionisation time-of-flight mass spectrometry

Appendix A

ELISA kits were used to measure serum levels of progesterone (MyBioSource, CA, USA, Cat. # MBS762170), estradiol (Cusabio Biotech Co., Wuhan, China; Cat. # CSB-E05110r), tumor necrosis factor-alpha (TNF-α; Cusabio Biotech Co., Wuhan, China; Cat. # CSB-E11897r), interleukin-1beta (IL-1β; MyBioSource, Vancouver, BC, Canada; Cat. # MBS825017) and cortical content of glial fibrillary acidic protein, brain-derived neurotrophic factor, and serotonin (GFAP, BDNF, and 5-HT; MyBioSource, Vancouver, BC, Canada; Cat. #MBS2505953, MBS824814, and MBS2700308, respectively) according to the manufacture directions.

Appendix B

The uterus samples collected from 2 rats/group in the dose selection part were fixed in buffered formaldehyde (10%); these samples were then embedded in paraffin wax to be sectioned using rotatory microtome. Samples were trimmed and processed by dehydration of samples in ethanol and cleared in xylene, to be stained either with Hematoxylin and Eosin (H&E) using a conventional light microscope [107].

Appendix C

MiReasy mini kit and methodology for purification of serum total RNA, involving MiR and long noncoding RNA, were used to extract RNA from uterine tissues (Qiagen, Valencia, CA, USA). The NanoDrop® (ND)-1000 spectrophotometer was used to quantify and assess the purity of RNA samples (NanoDrop Technologies, Inc. Wilmington, NC, USA).

For the detection of mature MiR-146a- and MiR-520, reverse transcription and quantitative real-time PCR (qPCR) were used. The miScript II RT kit was used to reverse transcript total RNA in a final volume of twenty uL RT reactions (Qiagen, Valencia, CA, USA).

In a total volume of 25 µL per reaction volume, quantitative RT-PCR was performed using the miScript SYBR® Green PCR kit and protocol for mature miRNAs quantitative assessment (Qiagen, Valencia, CA, USA) utilizing the specific MiR-(520 and 146a) primers. The PCR primers used are presented in Table S1. The fold change in MiRs expression were calculated by Equation $2-\Delta\Delta Ct$.

Appendix D

The RIPA fractions of the uterine homogenates were used for Western blot analyses as depicted formerly [108,109]. The primary Rabbit polyclonal antibodies were purchased from Thermo Scientific Co. (Waltham, MA, USA) of the following parameters: matrix metalloproteinase-9 and tissue inhibitor of metalloproteinase-1 (MMP-9, TIMP-1; Cat #PA5-13199, PA1-85923, respectively). Specific signals were developed with a Chem- iDocTM imaging system using Image LabTM software version 5.1 (Bio- Rad Laboratories Inc., Hercules, CA, USA). The optical density (OD) of the subsequently mentioned results was normalized to β-actin and total protein.

Appendix E

The analysis was carried out on an ExionLC analytical UHPLC system (SCIEX, Framingham, MA, USA) outfitted with a column (Waters, Xbridge C-18, 50 mm 2.1 mm, 3 m particle size) and precolumn (In-Line filter discs, Phenomenex, 0.5 m 3.0 mm). The following mobile phases were used: mobile phase (A) 5 mM ammonium formate buffer pH 3 in 1% methanol; mobile phase (B) 5 mM ammonium formate buffer pH 8 in 1% methanol; and mobile phase (C) 100% acetonitrile. Negative ion mode solvents (B) and (C) were used, while positive ion mode solvents (A) and (C) were used. Gradient elution was carried out at a flow rate of 0.3 mL/min. at 40 C, with isocratic (90% (A or B), 10% (C)), from 21–25 min, isocratic 10% (A) or (B), to 90% (C). From 25.01–28 min, elution was isocratic (90% (A or B), 10% (C)), until equilibrium was reached.

The mass spectrometry was performed on a Triple TOF 5600+ system equipped with an ESI mode and a Duo-Spray source (SCIEX, Concord, ON, Canada). The sprayer and declustering voltages were set to 4500 and 80 eV, respectively, in the positive ESI mode, and 4500 and 80 V in the negative ESI mode. The following parameters were used: source temperature of 600 °C, collision energy of 35 V/35 V in positive and negative modes, CE spreading of 20 V, and ion tolerance of 10 ppm. The IDA protocol (information-dependent acquisition) was used for Triple TOF 5600+ operation. MS/MS data were generated using the Analyst-TF 1.7.1 software. Full-scan MS and MS/MS data for high-resolution survey spectra ranging from 50 to 1100 m/z were obtained.

References

1. Ciganda, C.; Laborde, A. Herbal infusions used for induced abortion. *J. Toxicol. Clin. Toxicol.* **2003**, *41*, 235–239. [CrossRef] [PubMed]
2. Anwar, F.; Abbas, A.; Mehmood, T.; Gilani, A.H.; Rehman, N.u. Mentha: A genus rich in vital nutra-pharmaceuticals—A review. *Phytother. Res.* **2019**, *33*, 2548–2570. [CrossRef] [PubMed]
3. Teixeira, B.; Marques, A.; Ramos, C.; Batista, I.; Serrano, C.; Matos, O.; Neng, N.R.; Nogueira, J.M.; Saraiva, J.A.; Nunes, M.L. European pennyroyal (*Mentha pulegium*) from Portugal: Chemical composition of essential oil and antioxidant and antimicrobial properties of extracts and essential oil. *Ind. Crop. Prod.* **2012**, *36*, 81–87. [CrossRef]
4. Hadi, M.Y.; Hameed, I.H.; Ibraheam, I.A. *Mentha pulegium*: Medicinal uses, Anti-Hepatic, Antibacterial, Antioxidant effect and Analysis of Bioactive Natural Compounds: A Review. *Res. J. Pharm. Technol.* **2017**, *10*, 3580–3584. [CrossRef]
5. Abdelli, M.; Moghrani, H.; Aboun, A.; Maachi, R. Algerian *Mentha pulegium* L. leaves essential oil: Chemical composition, antimicrobial, insecticidal and antioxidant activities. *Ind. Crop. Prod.* **2016**, *94*, 197–205. [CrossRef]
6. Riddle, J.M. *Eve's Herbs: A History of Contraception and Abortion in the West*; Harvard University Press: Cambridge, MA, USA, 1997.
7. Schiebinger, L. *Plants and Empire*; Harvard University Press: Cambridge, MA, USA, 2021.
8. Marzouk, M.M.; Hussein, S.R.; Elkhateeb, A.; El-shabrawy, M.; Abdel-Hameed, E.-S.S.; Kawashty, S.A. Comparative study of Mentha species growing wild in Egypt: LC-ESI-MS analysis and chemosystematic significance. *J. Appl. Pharm. Sci.* **2018**, *8*, 116–122.

9. Taamalli, A.; Arráez-Román, D.; Abaza, L.; Iswaldi, I.; Fernández-Gutiérrez, A.; Zarrouk, M.; Segura-Carretero, A. LC-MS-based metabolite profiling of methanolic extracts from the medicinal and aromatic species *Mentha pulegium* and *Origanum majorana*. *Phytochem. Anal.* **2015**, *26*, 320–330. [CrossRef]
10. Blanchard, K.; Winikoff, B.; Ellertson, C. Misoprostol used alone for the termination of early pregnancy: A review of the evidence. *Contraception* **1999**, *59*, 209–217. [CrossRef]
11. Taher, E.; Swelam, M.; Mansy, A.; Elgammal, M. Methotrexate and Misoprostol against Misoprostol Alone for Early Medical Abortion: Comparative Study. *J. High Inst. Public Health* **2014**, *44*, 21–24. [CrossRef]
12. Moreno-Ruiz, N.; Borgatta, L.; Yanow, S.; Kapp, N.; Wiebe, E.; Winikoff, B. Alternatives to mifepristone for early medical abortion. *Int. J. Gynecol. Obstet.* **2007**, *96*, 212–218. [CrossRef]
13. Fouche-Camargo, J.S. Uterotonics and tocolytics. In *Clinical Pharmacology during Pregnancy*; Elsevier: Amsterdam, The Netherlands, 2022; pp. 323–338.
14. Shokrzadeh, M.; Dashti, A.; Aghajanshakeri, S.; Pourabbas, B.; Ghassemi Barghi, N.; Ogunkunle, A. Prevention effects of *Foeniculum vulgare* (Fennel) hydroalcoholic extract for threatened abortion by misoprostol induction in experimental mice. *Int. J. Trad. Nat. Med.* **2019**, *9*, 1–16.
15. Auffret, M.; Bernard-Phalippon, N.; Dekemp, J.; Carlier, P.; Boyer, M.G.; Vial, T.; Gautier, S. Misoprostol exposure during the first trimester of pregnancy: Is the malformation risk varying depending on the indication? *Eur. J. Obstet. Gynecol. Reprod. Biol.* **2016**, *207*, 188–192. [CrossRef] [PubMed]
16. Barbero, P.; Liascovich, R.; Valdez, R.; Moresco, A. Misoprostol teratogenicity: A prospective study in Argentina. *Arch. Argent. Pediatr.* **2011**, *109*, 226–231.
17. Kazuno, S.; Yanagida, M.; Shindo, N.; Murayama, K. Mass spectrometric identification and quantification of glycosyl flavonoids, including dihydrochalcones with neutral loss scan mode. *Anal. Biochem.* **2005**, *347*, 182–192. [CrossRef]
18. Jiang, R.-W.; Lau, K.-M.; Hon, P.-M.; Mak, T.C.; Woo, K.-S.; Fung, K.-P. Chemistry and biological activities of caffeic acid derivatives from Salvia miltiorrhiza. *Curr. Med. Chem.* **2005**, *12*, 237–246. [CrossRef]
19. Farag, M.A.; Rasheed, D.M.; Kropf, M.; Heiss, A.G. Metabolite profiling in Trigonella seeds via UPLC-MS and GC-MS analyzed using multivariate data analyses. *Anal. Bioanal. Chem.* **2016**, *408*, 8065–8078. [CrossRef]
20. Otify, A.M.; El-Sayed, A.M.; Michel, C.G.; Farag, M.A. Metabolites profiling of date palm (Phoenix dactylifera L.) commercial by-products (pits and pollen) in relation to its antioxidant effect: A multiplex approach of MS and NMR metabolomics. *Metabolomics* **2019**, *15*, 119. [CrossRef]
21. Jebali, J.; Ghazghazi, H.; Aouadhi, C.; ELBini-Dhouib, I.; Ben Salem, R.; Srairi-Abid, N.; Marrakchi, N.; Rigane, G. Tunisian Native *Mentha pulegium* L. Extracts: Phytochemical Composition and Biological Activities. *Molecules* **2022**, *27*, 314. [CrossRef]
22. Zhang, A.; Sun, H.; Yan, G.; Wang, X. Recent developments and emerging trends of mass spectrometry for herbal ingredients analysis. *TrAC Trends Anal. Chem.* **2017**, *94*, 70–76. [CrossRef]
23. Hajlaouia, H.; Mighrib, H.; Hamdauic, G.; Aounia, M. Antioxidant activities and RP-HPLC identification of polyphenols in the methanolic extract of Mentha genus. *Tunis. J. Med. Plants Nat. Prod. (TJMPNP)* **2015**, *14*, 1–11.
24. Sellami, I.H.; Maamouri, E.; Chahed, T.; Wannes, W.A.; Kchouk, M.E.; Marzouk, B. Effect of growth stage on the content and composition of the essential oil and phenolic fraction of sweet marjoram (*Origanum majorana* L.). *Ind. Crops Prod.* **2009**, *30*, 395–402. [CrossRef]
25. Buckingham, J. *Dictionary of Natural Products, Supplement 4*; CRC Press: Boca Raton, FL, USA, 1997; Volume 11.
26. Loussouarn, M.; Krieger-Liszkay, A.; Svilar, L.; Bily, A.; Birtić, S.; Havaux, M. Carnosic acid and carnosol, two major antioxidants of rosemary, act through different mechanisms. *Plant Physiol.* **2017**, *175*, 1381–1394. [CrossRef] [PubMed]
27. Guerrero, I.C.; Andrés, L.S.; León, L.G.; Machín, R.P.; Padrón, J.M.; Luis, J.G.; Delgadillo, J. Abietane diterpenoids from *Salvia pachyphylla* and *S. clevelandii* with cytotoxic activity against human cancer cell lines. *J. Nat. Prod.* **2006**, *69*, 1803–1805. [CrossRef] [PubMed]
28. Wang, D.; Yu, W.; Cao, L.; Xu, C.; Tan, G.; Zhao, Z.; Huang, M.; Jin, J. Comparative pharmacokinetics and tissue distribution of cryptotanshinone, tanshinone IIA, dihydrotanshinone I, and tanshinone I after oral administration of pure tanshinones and liposoluble extract of *Salvia miltiorrhiza* to rats. *Biopharm. Drug Dispos.* **2020**, *41*, 54–63. [CrossRef] [PubMed]
29. Nair, S.N.; Menon, S.; Shailajan, S. A liquid chromatography/electrospray ionization tandem mass spectrometric method for quantification of asiatic acid from plasma: Application to pharmacokinetic study in rats. *Rapid Commun. Mass Spectrom.* **2012**, *26*, 1899–1908. [CrossRef]
30. Shen, D.; Pan, M.-H.; Wu, Q.-L.; Park, C.-H.; Juliani, H.R.; Ho, C.-T.; Simon, J.E. LC-MS method for the simultaneous quantitation of the anti-inflammatory constituents in oregano (*Origanum* species). *J. Agric. Food Chem.* **2010**, *58*, 7119–7125. [CrossRef]
31. Basal, W.T.; Ahmed, A.R.T.; Mahmoud, A.A.; Omar, A.R. Lufenuron induces reproductive toxicity and genotoxic effects in pregnant albino rats and their fetuses. *Sci. Rep.* **2020**, *10*, 19544. [CrossRef]
32. Mesiano, S. Roles of estrogen and progesterone in human parturition. *Endocrinol. Parturition* **2001**, *27*, 86–104.
33. Bridges, R.S. A quantitative analysis of the roles of dosage, sequence, and duration of estradiol and progesterone exposure in the regulation of maternal behavior in the rat. *Endocrinology* **1984**, *114*, 930–940. [CrossRef]
34. Amadi, C.N.; Igweze, Z.N.; Orisakwe, O.E. Heavy metals in miscarriages and stillbirths in developing nations. *Middle East Fertil. Soc. J.* **2017**, *22*, 91–100. [CrossRef]

35. Wang, X.; Chen, X.; Feng, X.; Chang, F.; Chen, M.; Xia, Y.; Chen, L. Triclosan causes spontaneous abortion accompanied by decline of estrogen sulfotransferase activity in humans and mice. *Sci. Rep.* **2015**, *5*, 18252. [CrossRef] [PubMed]
36. Obernosterer, G.; Leuschner, P.J.; Alenius, M.; Martinez, J. Post-transcriptional regulation of microRNA expression. *RNA* **2006**, *12*, 1161–1167. [CrossRef] [PubMed]
37. Cai, M.; Kolluru, G.K.; Ahmed, A. Small molecule, big prospects: microRNA in pregnancy and its complications. *J. Pregnancy* **2017**, *2017*, 6972732. [CrossRef] [PubMed]
38. Timofeeva, A.V.; Gusar, V.A.; Kan, N.E.; Prozorovskaya, K.N.; Karapetyan, A.O.; Bayev, O.R.; Chagovets, V.V.; Kliver, S.F.; Iakovishina, D.Y.; Frankevich, V.E. Identification of potential early biomarkers of preeclampsia. *Placenta* **2018**, *61*, 61–71. [CrossRef] [PubMed]
39. Ye, H.-x.; Li, L.; Dong, Y.-j.; Li, P.-h.; Su, Q.; Guo, Y.-h.; Lu, Y.-r.; Zhong, Y.; Jia, Y.; Cheng, J.-q. miR-146a-5p improves the decidual cytokine microenvironment by regulating the toll-like receptor signaling pathway in unexplained spontaneous abortion. *Int. Immunopharmacol.* **2020**, *89*, 107066. [CrossRef]
40. Sang, Q.; Yao, Z.; Wang, H.; Feng, R.; Wang, H.; Zhao, X.; Xing, Q.; Jin, L.; He, L.; Wu, L. Identification of microRNAs in human follicular fluid: Characterization of microRNAs that govern steroidogenesis in vitro and are associated with polycystic ovary syndrome in vivo. *J. Clin. Endocrinol. Metab.* **2013**, *98*, 3068–3079. [CrossRef]
41. Yuan, D.-z.; Yu, L.-l.; Qu, T.; Zhang, S.-m.; Zhao, Y.-b.; Pan, J.-l.; Xu, Q.; He, Y.-p.; Zhang, J.-h.; Yue, L.-m. Identification and characterization of progesterone-and estrogen-regulated MicroRNAs in mouse endometrial epithelial cells. *Reprod. Sci.* **2015**, *22*, 223–234. [CrossRef]
42. Zhang, Y.; Li, P.; Guo, Y.; Liu, X.; Zhang, Y. MMP-9 and TIMP-1 in placenta of hypertensive disorder complicating pregnancy. *Exp. Ther. Med.* **2019**, *18*, 637–641. [CrossRef]
43. Chen, J.; Khalil, R.A. Matrix metalloproteinases in normal pregnancy and preeclampsia. *Prog. Mol. Biol. Transl. Sci.* **2017**, *148*, 87–165.
44. Laskowska, M. Altered maternal serum matrix metalloproteinases MMP-2, MMP-3, MMP-9, and MMP-13 in severe early-and late-onset preeclampsia. *BioMed Res. Int.* **2017**, *2017*, 6432426. [CrossRef]
45. Dang, Y.; Li, W.; Tran, V.; Khalil, R.A. EMMPRIN-mediated induction of uterine and vascular matrix metalloproteinases during pregnancy and in response to estrogen and progesterone. *Biochem. Pharmacol.* **2013**, *86*, 734–747. [CrossRef] [PubMed]
46. Mönckedieck, V.; Sannecke, C.; Husen, B.; Kumbartski, M.; Kimmig, R.; Tötsch, M.; Winterhager, E.; Grümmer, R. Progestins inhibit expression of MMPs and of angiogenic factors in human ectopic endometrial lesions in a mouse model. *Mol. Hum. Reprod.* **2009**, *15*, 633–643. [CrossRef] [PubMed]
47. Kalagiri, R.R.; Carder, T.; Choudhury, S.; Vora, N.; Ballard, A.R.; Govande, V.; Drever, N.; Beeram, M.R.; Uddin, M.N. Inflammation in complicated pregnancy and its outcome. *Am. J. Perinatol.* **2016**, *33*, 1337–1356. [CrossRef] [PubMed]
48. Christiansen, O.B.; Nielsen, H.S.; Kolte, A.M. Seminars in Fetal and Neonatal Medicine. In *Inflammation and Miscarriage*; Elsevier: Amsterdam, The Netherlands, 2006; pp. 302–308.
49. Ginsberg, Y.; Khatib, N.; Weiner, Z.; Beloosesky, R. Maternal inflammation, fetal brain implications and suggested neuroprotection: A summary of 10 years of research in animal models. *Rambam Maimonides Med. J.* **2017**, *8*, e0028. [CrossRef]
50. Schreiber, K.; Sciascia, S.; De Groot, P.G.; Devreese, K.; Jacobsen, S.; Ruiz-Irastorza, G.; Salmon, J.E.; Shoenfeld, Y.; Shovman, O.; Hunt, B.J. Antiphospholipid syndrome. *Nat. Rev. Dis. Primers* **2018**, *4*, 17103. [CrossRef]
51. Cotechini, T.; Komisarenko, M.; Sperou, A.; Macdonald-Goodfellow, S.; Adams, M.A.; Graham, C.H. Inflammation in rat pregnancy inhibits spiral artery remodeling leading to fetal growth restriction and features of preeclampsia. *J. Exp. Med.* **2014**, *211*, 165–179. [CrossRef]
52. Romero, R.; Durum, S.; Dinarello, C.; Hobbins, J.; Mitchell, M. Interleukin-1: A Signal for the Initiation of Labor in Chorioamnionitis. In Proceedings of the 33rd Annual Meeting for the Society for Gynecologic Investigation, Toronto, ON, Canada, 19–22 March 1986; pp. 19–22.
53. Pařízek, A.; Koucký, M.; Dušková, M. Progesterone, inflammation and preterm labor. *J. Steroid Biochem. Mol. Biol.* **2014**, *139*, 159–165. [CrossRef]
54. He, Y.; Sun, Q. IFN-γ induces upregulation of TNF-α, downregulation of MMP-2 and MMP-9 expressions in abortion rat. *Eur. Rev. Med. Pharm. Sci.* **2018**, *22*, 4762–4767.
55. Trentini, A.; Maritati, M.; Cervellati, C.; Manfrinato, M.C.; Gonelli, A.; Volta, C.A.; Vesce, F.; Greco, P.; Dallocchio, F.; Bellini, T. Vaginal lactoferrin modulates PGE2, MMP-9, MMP-2, and TIMP-1 amniotic fluid concentrations. *Mediat. Inflamm.* **2016**, *2016*, 3648719. [CrossRef]
56. Marinescu, I.P.; Foarfa, M.C.; Pirlog, M.-C.; Turculeanu, A. Prenatal depression and stress-risk factors for placental pathology and spontaneous abortion. *Romanian J. Morphol. Embryol.* **2014**, *55* (Suppl. S3), 1155–1160.
57. Fergusson, D.M.; Horwood, L.J.; Boden, J.M. Abortion and mental health disorders: Evidence from a 30-year longitudinal study. *Br. J. Psychiatry* **2008**, *193*, 444–451. [CrossRef] [PubMed]
58. Luo, M.; Jiang, X.; Wang, Y.; Wang, Z.; Shen, Q.; Li, R.; Cai, Y. Association between induced abortion and suicidal ideation among unmarried female migrant workers in three metropolitan cities in China: A cross-sectional study. *BMC Public Health* **2018**, *18*, 625. [CrossRef] [PubMed]
59. Reardon, D.C. The abortion and mental health controversy: A comprehensive literature review of common ground agreements, disagreements, actionable recommendations, and research opportunities. *SAGE Open Med.* **2018**, 6. [CrossRef] [PubMed]

60. Gould, T.D.; Dao, D.; Kovacsics, C. *Mood and Anxiety Related Phenotypes in Mice: Characterization Using Behavioral Tests*; Springer: Berlin/Heidelberg, Germany, 2009; Volume 2.
61. Zhang, T.; Zheng, X.; Wang, X.; Zhao, H.; Wang, T.; Zhang, H.; Li, W.; Shen, H.; Yu, L. Maternal exposure to PM2. 5 during pregnancy induces impaired development of cerebral cortex in mice offspring. *Int. J. Mol. Sci.* **2018**, *19*, 257. [CrossRef] [PubMed]
62. Zhang, X.; Li, H.; Sun, H.; Jiang, Y.; Wang, A.; Kong, Y.; Sun, X.; Zhu, G.; Li, Q.; Du, Z. Effects of BDNF signaling on anxiety-related behavior and spatial memory of adolescent rats in different length of maternal separation. *Front. Psychiatry* **2020**, *11*, 709. [CrossRef] [PubMed]
63. Zimcikova, E.; Simko, J.; Karesova, I.; Kremlacek, J.; Malakova, J. Behavioral effects of antiepileptic drugs in rats: Are the effects on mood and behavior detectable in open-field test? *Seizure* **2017**, *52*, 35–40. [CrossRef]
64. Sestakova, N.; Puzserova, A.; Kluknavsky, M.; Bernatova, I. Determination of motor activity and anxiety-related behaviour in rodents: Methodological aspects and role of nitric oxide. *Interdiscip. Toxicol.* **2013**, *6*, 126–135. [CrossRef]
65. Christakis, D.A.; Ramirez, J.S.; Ramirez, J.-M. Overstimulation of newborn mice leads to behavioral differences and deficits in cognitive performance. *Sci. Rep.* **2012**, *2*, 546. [CrossRef]
66. Lopatina, O.; Yoshihara, T.; Nishimura, T.; Zhong, J.; Akther, S.; Fakhrul, A.A.; Liang, M.; Higashida, C.; Sumi, K.; Furuhara, K. Anxiety-and depression-like behavior in mice lacking the CD157/BST1 gene, a risk factor for Parkinson's disease. *Front. Behav. Neurosci.* **2014**, *8*, 133. [CrossRef]
67. Nynas, J.; Narang, P.; Kolikonda, M.K.; Lippmann, S. Depression and anxiety following early pregnancy loss: Recommendations for primary care providers. *Prim. Care Companion CNS Disord.* **2015**, *17*, 26225. [CrossRef]
68. Gómora-Arrati, P.; González-Arenas, A.; Balandrán-Ruiz, M.A.; Mendoza-Magaña, M.L.; González-Flores, O.; Camacho-Arroyo, I. Changes in the content of GFAP in the rat brain during pregnancy and the beginning of lactation. *Neurosci. Lett.* **2010**, *484*, 197–200. [CrossRef] [PubMed]
69. Kinsley, C.H.; Lambert, K.G. Reproduction-induced neuroplasticity: Natural behavioural and neuronal alterations associated with the production and care of offspring. *J. Neuroendocrinol.* **2008**, *20*, 515–525. [CrossRef] [PubMed]
70. Scott, H.; Phillips, T.J.; Stuart, G.C.; Rogers, M.F.; Steinkraus, B.R.; Grant, S.; Case, C.P. Preeclamptic placentae release factors that damage neurons: Implications for foetal programming of disease. *Neuronal Signal.* **2018**, *2*, NS20180139. [CrossRef] [PubMed]
71. Dingsdale, H.; Nan, X.; Garay, S.M.; Mueller, A.; Sumption, L.A.; Chacón-Fernández, P.; Martinez-Garay, I.; Ghevaert, C.; Barde, Y.-A.; John, R.M. The placenta protects the fetal circulation from anxiety-driven elevations in maternal serum levels of brain-derived neurotrophic factor. *Transl. Psychiatry* **2021**, *11*, 62. [CrossRef] [PubMed]
72. Begliuomini, S.; Casarosa, E.; Pluchino, N.; Lenzi, E.; Centofanti, M.; Freschi, L.; Pieri, M.; Genazzani, A.; Luisi, S.; Genazzani, A.R. Influence of endogenous and exogenous sex hormones on plasma brain-derived neurotrophic factor. *Hum. Reprod.* **2007**, *22*, 995–1002. [CrossRef]
73. Wessels, J.M.; Leyland, N.A.; Agarwal, S.K.; Foster, W.G. Estrogen induced changes in uterine brain-derived neurotrophic factor and its receptors. *Hum. Reprod.* **2015**, *30*, 925–936. [CrossRef]
74. Blakeley, P.M.; Capron, L.E.; Jensen, A.B.; O'Donnell, K.J.; Glover, V. Maternal prenatal symptoms of depression and down regulation of placental monoamine oxidase A expression. *J. Psychosom. Res.* **2013**, *75*, 341–345. [CrossRef]
75. Del Río, J.P.; Alliende, M.I.; Molina, N.; Serrano, F.G.; Molina, S.; Vigil, P. Steroid hormones and their action in women's brains: The importance of hormonal balance. *Front. Public Health* **2018**, *6*, 141. [CrossRef]
76. Bennetts, H.; Underwood, E.; Shier, F.L. A specific breeding problem of sheep on subterranean clover pastures in Western Australia. *Vet. J.* **1946**, *102*, 348–352.
77. Cos, P.; De Bruyne, T.; Apers, S.; Berghe, D.V.; Pieters, L.; Vlietinck, A.J. Phytoestrogens: Recent developments. *Planta Med.* **2003**, *69*, 589–599.
78. Basly, J.-P.; Lavier, M.-C.C. Dietary phytoestrogens: Potential selective estrogen enzyme modulators? *Planta Med.* **2005**, *71*, 287–294. [CrossRef] [PubMed]
79. Al-Fartosi, K.G.; Al-Rekabi, E.A. Effect of phenolic compounds of leaves extractes from *Mentha spicata* and *Mentha longifolia* on sex hormones level of female rats. *J. Coll. Educ. Pure Sci.* **2012**, *2*, 118–126.
80. Jung, B.I.; Kim, M.S.; Kim, H.A.; Kim, D.; Yang, J.; Her, S.; Song, Y.S. Caffeic acid phenethyl ester, a component of beehive propolis, is a novel selective estrogen receptor modulator. *Phytother. Res. Int. J. Devoted Pharmacol. Toxicol. Eval. Nat. Prod. Deriv.* **2010**, *24*, 295–300. [CrossRef] [PubMed]
81. Ekeuku, S.O.; Pang, K.-L.; Chin, K.-Y. Effects of caffeic acid and its derivatives on bone: A systematic review. *Drug Des. Dev. Ther.* **2021**, *15*, 259. [CrossRef]
82. Zych, M.; Kaczmarczyk-Sedlak, I.; Wojnar, W.; Folwarczna, J. Effect of rosmarinic acid on the serum parameters of glucose and lipid metabolism and oxidative stress in estrogen-deficient rats. *Nutrients* **2019**, *11*, 267. [CrossRef]
83. Ghasemzadeh, A.; Khaki, A.; Farzadi, L.; Khaki, A.; Marjani, M.; Ashteani, H.A.; Hamdi, B.A.; Ghadamkheir, E.; Naeimikararoudi, M.; Ouladsahebmadarek, E. Effect of rosmarinic acid on estrogen, FSH and LH in female diabetic rats. *Afr. J. Pharm. Pharmacol.* **2011**, *5*, 1427–1431. [CrossRef]
84. Aliyev, A.; Ozcan-Sezer, S.; Akdemir, A.; Gurer-Orhan, H. In vitro evaluation of estrogenic, antiestrogenic and antitumor effects of amentoflavone. *Hum. Exp. Toxicol.* **2021**, *40*, 1510–1518. [CrossRef]

85. Sanderson, J.T.; Hordijk, J.; Denison, M.S.; Springsteel, M.F.; Nantz, M.H.; Van Den Berg, M. Induction and inhibition of aromatase (CYP19) activity by natural and synthetic flavonoid compounds in H295R human adrenocortical carcinoma cells. *Toxicol. Sci.* **2004**, *82*, 70–79. [CrossRef]
86. Wei, Y.; Yuan, P.; Zhang, Q.; Fu, Y.; Hou, Y.; Gao, L.; Zheng, X.; Feng, W. Acacetin improves endothelial dysfunction and aortic fibrosis in insulin-resistant SHR rats by estrogen receptors. *Mol. Biol. Rep.* **2020**, *47*, 6899–6918. [CrossRef]
87. Vitale, D.C.; Piazza, C.; Melilli, B.; Drago, F.; Salomone, S. Isoflavones: Estrogenic activity, biological effect and bioavailability. *Eur. J. Drug Metab. Pharmacokinet.* **2013**, *38*, 15–25. [CrossRef]
88. Nynca, A.; Słonina, D.; Jabłońska, O.; Kamińska, B.; Ciereszko, R. Daidzein affects steroidogenesis and oestrogen receptor expression in medium ovarian follicles of pigs. *Acta Vet. Hung.* **2013**, *61*, 85–98. [CrossRef] [PubMed]
89. Yang, X.; Jiang, Y.; Yang, J.; He, J.; Sun, J.; Chen, F.; Zhang, M.; Yang, B. Prenylated flavonoids, promising nutraceuticals with impressive biological activities. *Trends Food Sci. Technol.* **2015**, *44*, 93–104. [CrossRef]
90. Botta, B.; Vitali, A.; Menendez, P.; Misiti, D.; Monache, G.D. Prenylated flavonoids: Pharmacology and biotechnology. *Curr. Med. Chem.* **2005**, *12*, 713–739. [CrossRef] [PubMed]
91. Milligan, S.R.; Kalita, J.C.; Pocock, V.; Van De Kauter, V.; Stevens, J.F.; Deinzer, M.L.; Rong, H.; De Keukeleire, D. The endocrine activities of 8-prenylnaringenin and related hop (*Humulus lupulus* L.) flavonoids. *J. Clin. Endocrinol. Metab.* **2000**, *85*, 4912–4915. [CrossRef]
92. Weng, X.C.; Gordon, M.H. Antioxidant activity of quinones extracted from tanshen (*Salvia miltiorrhiza* Bunge). *J. Agric. Food Chem.* **1992**, *40*, 1331–1336. [CrossRef]
93. Xu, S.; Liu, P. Tanshinone II-A: New perspectives for old remedies. *Expert Opin. Ther. Pat.* **2013**, *23*, 149–153. [CrossRef] [PubMed]
94. Nwankudu, N.; Ndibe, N.; Ijioma, S. Oxytocic effect of Ananas comosus fruit juice on isolated pregnant rats uteri. *Niger. Vet. J.* **2015**, *36*, 1318–1326.
95. Ochiogu, I.S.; Uchendu, C.N.; Ihedioha, J.I. A new and simple method of confirmatory detection of mating in albino rats (*Rattus norvegicus*). *Anim. Res. Int.* **2006**, *3*, 527–530. [CrossRef]
96. Shibeshi, W.; Makonnen, E.; Zerihun, L.; Debella, A. Effect of Achyranthes aspera L. on fetal abortion, uterine and pituitary weights, serum lipids and hormones. *Afr. Health Sci.* **2006**, *6*, 108–112.
97. Li, L.; Huang, Q.; Duan, X.; Han, L.; Peng, D. Protective effect of *Clinopodium chinense* (Benth.) O. Kuntze against abnormal uterine bleeding in female rats. *J. Pharmacol. Sci.* **2020**, *143*, 1–8. [CrossRef]
98. Marcondes, F.; Bianchi, F.; Tanno, A. Determination of the estrous cycle phases of rats: Some helpful considerations. *Braz. J. Biol.* **2002**, *62*, 609–614. [CrossRef] [PubMed]
99. Camilleri, C.; Beiter, R.M.; Puentes, L.; Aracena-Sherck, P.; Sammut, S. Biological, behavioral and physiological consequences of drug-induced pregnancy termination at first-trimester human equivalent in an animal model. *Front. Neurosci.* **2019**, *13*, 544. [CrossRef] [PubMed]
100. Stramek, A.K.; Johnson, M.L.; Taylor, V.J. Improved timed-mating, non-invasive method using fewer unproven female rats with pregnancy validation via early body mass increases. *Lab. Anim.* **2019**, *53*, 148–159. [CrossRef] [PubMed]
101. Namulindwa, A.; Nkwangu, D.; Oloro, J. Determination of the abortifacient activity of the aqueous extract of *Phytolacca dodecandra* (LHer) leaf in Wistar rats. *Afr. J. Pharm. Pharmacol.* **2015**, *9*, 43–47.
102. Paylor, R.; Spencer, C.M.; Yuva-Paylor, L.A.; Pieke-Dahl, S. The use of behavioral test batteries, II: Effect of test interval. *Physiol. Behav.* **2006**, *87*, 95–102. [CrossRef]
103. Elfouly, A.; Awny, M.; Ibrahim, M.; Aboelsaad, M.; Tian, J.; Sayed, M. Effects of Long-Acting Testosterone Undecanoate on Behavioral Parameters and Na^+, K^+-ATPase mRNA Expression in Mice with Alzheimers Disease. *Neurochem. Res.* **2021**, *46*, 2238–2248. [CrossRef]
104. Rojas-Carvajal, M.; Fornaguera, J.; Mora-Gallegos, A.; Brenes, J.C. Testing experience and environmental enrichment potentiated open-field habituation and grooming behaviour in rats. *Anim. Behav.* **2018**, *137*, 225–235. [CrossRef]
105. Emad, A.M.; Rasheed, D.M.; El-Kased, R.F.; El-Kersh, D.M. Antioxidant, Antimicrobial Activities and Characterization of Polyphenol-Enriched Extract of Egyptian Celery (*Apium graveolens* L., Apiaceae) Aerial Parts via UPLC/ESI/TOF-MS. *Molecules* **2022**, *27*, 698. [CrossRef]
106. Rasheed, D.M.; Emad, A.M.; Ali, S.F.; Ali, S.S.; Farag, M.A.; Meselhy, M.R.; Sattar, E.A. UPLC-PDA-ESI/MS metabolic profiling of dill shoots bioactive fraction; evidence of its antioxidant and hepatoprotective effects in vitro and in vivo. *J. Food Biochem.* **2021**, *45*, e13741. [CrossRef]
107. Bancroft, J.D.; Stevens, A. *Theory and Practice of Histological Techniques*, 4th ed.; Churchill Livingstone: New York, NY, USA, 1996.
108. Soubh, A.A.; El-Gazar, A.A.; Mohamed, E.A.; Awad, A.S.; El-Abhar, H.S. Further insights for the role of Morin in mRTBI: Implication of non-canonical Wnt/PKC-α and JAK-2/STAT-3 signaling pathways. *Int. Immunopharmacol.* **2021**, *100*, 108123. [CrossRef]
109. Ji, J.; Zhang, R.; Li, H.; Zhu, J.; Pan, Y.; Guo, Q. Analgesic and anti-inflammatory effects and mechanism of action of borneol on photodynamic therapy of acne. *Environ. Toxicol. Pharmacol.* **2020**, *75*, 103329. [CrossRef] [PubMed]